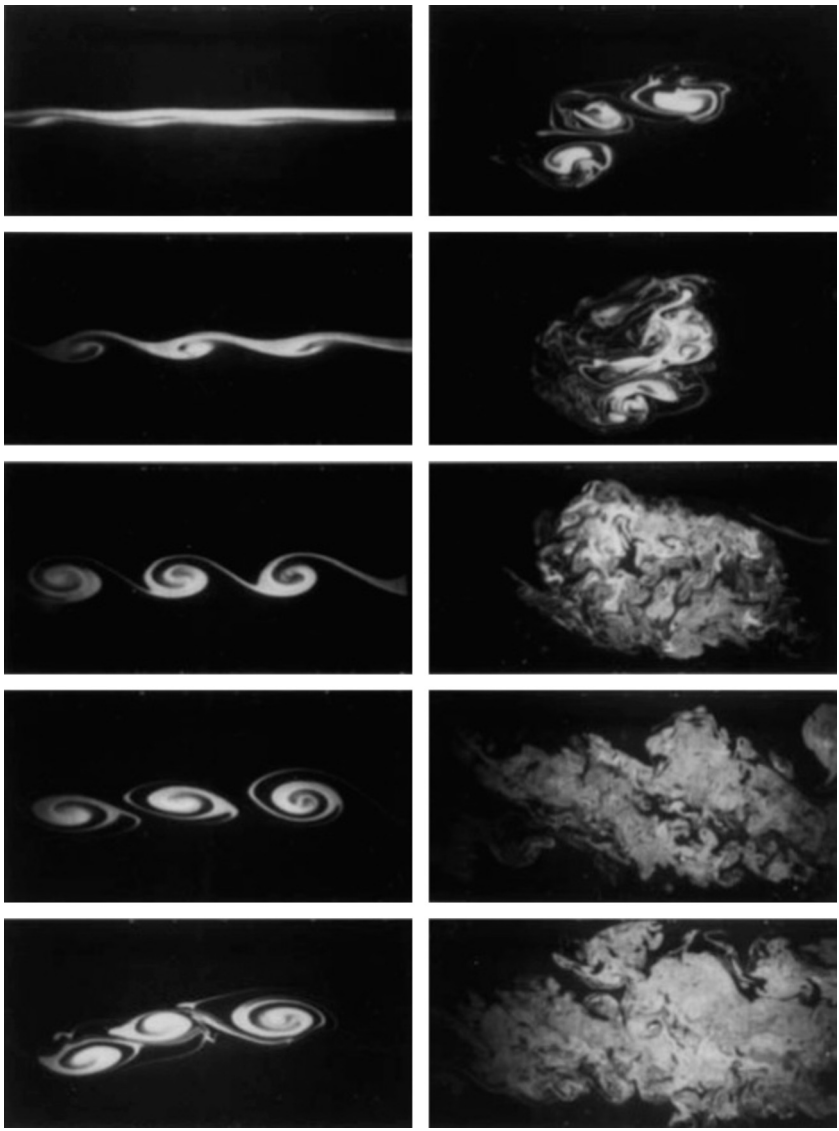

Transition to turbulence by Kelvin-Helmholtz instability in a shear flow. Reproduced from Falkovich, G., Sreenivasan, K.R., 2006, Lessons from hydrodynamic turbulence. Physics Today 59(4), 43–49, with the permission of the American Institute of Physics

Chapter 7

Vorticity Dynamics

In fact, a tornado is created by the inability of a funnel cloud to separate from the main cloud. It is caused by the resistance to the eddy when it is dragged on the earth, attached but unable to separate from the cloud. Thus, when the vortex propagates in a straight line, it moves violently in a circular motion everything it encounters.

Aristotle. Meteorologica 371 a., 9–15

Free-Surface Flow. DOI: 10.1016/B978-0-12-815489-2.00007-1

7.1 INTRODUCTION

In ideal fluid flow, our analysis was based on the assumption that the velocity field, $\mathbf{V}(\mathbf{x}, t)$, was generated from a velocity potential, which precluded the presence of rotation in the flow field. In viscous fluids, however, in addition to the velocity, the vorticity of the fluid, defined by Eq. (5.86), carries important information about the behavior of the flow. It is tempting to associate the existence of vorticity with the presence of a visible swirling flow pattern, as is the case of a *sink vortex* encountered when a body of water empties from an opening at the bottom of a large reservoir. Observations show that at large distances from the drain, the angular velocity vanishes while it attains very high values near the center of the vortex in order to conserve angular momentum. It turns out, however, that with the exception of its center, this common vortex actually has no vorticity. Therefore, although vorticity is intricately related to the velocity field, the interaction is not as simple as it appears at first. Not only is vorticity produced by the current, but vorticity can induce a stream itself. Furthermore, when the velocity and vorticity vectors are aligned, some remarkable flow patterns are created.

Although vorticity can be present in laminar flow, vorticity is of central importance in turbulence. It is actually impossible to imagine turbulence without flow rotation. One mechanism for the generation of turbulence is the creation of an instability in shear flow between two layers of fluid, known as *Kelvin-Helmholtz instability*. This is shown in the experiment captured by a series of photographs in the introduction figure of this chapter where part of the fluid near the interface between the two layers is colored with a dye. As the dye is sheared by the opposing uniform streams of fluid, roll waves appear on the interface. As time elapses, the waves evolve into distinct vortices that eventually merge with other vortices. Finally, small scale structures appear in the flow, which make up what we call turbulence (Falkovich and Sreenivasan, 2006). The actual physics of this process is not perfectly understood, but the role of vorticity seems crucial.

7.1.1 Vortex Lines

Let us try to visualize a vorticity vector field superimposed on the velocity vector field. In the same way that we imagined the flow field traversed by streamlines tangent to the velocity vector at every point, we can also envision the entire fluid space threaded by *vortex lines* that are tangent to the vorticity vector field. The vortex lines are aligned along the local axis of spin of the fluid particles and, in two-dimensional or axi-symmetric flows, the vortex lines are orthogonal to the streamlines. The equations describing the vortex lines can be written, in analogy to Eq. (2.67), as follows

$$\frac{dx}{\omega_x} = \frac{dy}{\omega_y} = \frac{dz}{\omega_z} \tag{7.1}$$

The physical rules that govern vortex lines are similar to those for streamlines. For example, vortex lines can never intersect. In the same way streamlines form stream tubes, as described in section 2.6.1, if we draw a vortex line through every point of a small closed curve, which is not itself a vortex line, we mark out a tube, which is called a *vortex tube*, as shown in Fig. 7.1. Finally, in analogy to a stream filament, a vortex tube whose cross-sectional area approaches zero is called a *vortex filament*.

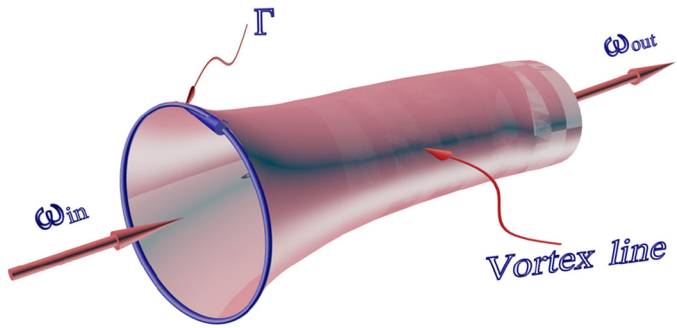

FIGURE 7.1 Vortex tube

In many applications, rotational flows can be described most efficiently in cylindrical coordinates (r, θ, z). In a cylindrical coordinate system, the velocity vector can be written as follows

$$\mathbf{V} = v_r \mathbf{r} + v_\theta \boldsymbol{\theta} + v_z \mathbf{k} \tag{7.2}$$

where v_r is the radial component of velocity, v_θ is the tangential component, and v_z is the axial component. Then, the curl of the velocity vector field in cylindrical coordinates can be found by replacing the generic vector in Eqs. (2.40) by Eq. (7.2). The result reads

$$\nabla_r \times \mathbf{V} = \left(\frac{1}{r}\frac{\partial v_z}{\partial \theta} - \frac{\partial v_\theta}{\partial z}\right)\mathbf{r} + \left(\frac{\partial v_r}{\partial z} - \frac{\partial v_z}{\partial r}\right)\boldsymbol{\theta} + \frac{1}{r}\left[\frac{\partial}{\partial r}(r v_\theta) - \frac{\partial v_r}{\partial \theta}\right]\mathbf{k} \tag{7.3}$$

7.1.2 Visualization of Vorticity

Vorticity is not intuitively identified or directly observable. In some cases the presence of vorticity is actually unexpected while in others it is surprisingly absent. This is explained by recalling that it is the **local** spin of a fluid particle that generates vorticity rather than the rigid body rotation of a fluid mass, in which particles do not move relative to each other.

The easiest way to detect the vorticity of the flow in the laboratory is to use a floating device such as a paddle wheel or a custom made *vorticity meter* (Shapiro, 1969). As shown in Fig. 7.2, the meter consists of two vanes attached

permanently at right angles, thus they form a paddle wheel. It is connected to a glass tube that can assist the device to float vertically. An arrow at the top of the tube shows the average rate of rotation. Therefore, if the paddle wheel turns about its own axis, we conclude that the flow is rotational and that the vorticity field is non-zero. The first vorticity meter was constructed by the Russian hydraulic engineer A.Ya. Milovich in 1913. He attached four blades to a cork, and observed the vorticity of the water in a channel bend (Joukovsky, 1914).

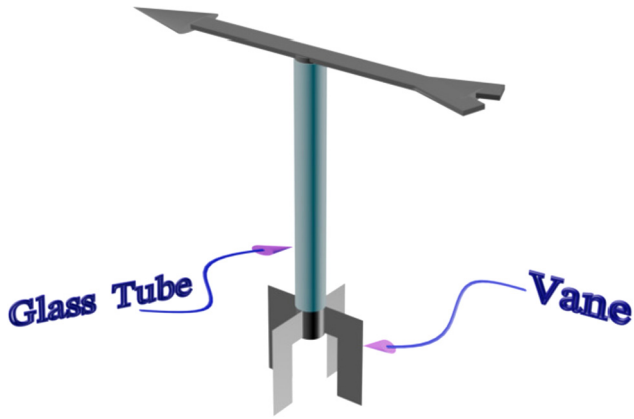

FIGURE 7.2 Vorticity meter

In many environmental and geophysical flows, vorticity can become organized, in which case vortices may become visible to an observer. Vorticity can also be disorganized and difficult to observe unless a vorticity meter or similar small paddle wheel is inserted in the flow. As mentioned earlier, although vorticity and rotation are intimately related, the absence of visible rotation in the flow does not preclude the generation of vorticity, as it is shown next.

7.2 VORTICITY IN SHEAR FLOW

Vorticity is an indicator of swirling in the flow, but the generation of vorticity is not always obvious. Consider, for example, the flow next to a solid boundary, as shown in Fig. 7.3. The streamlines are straight lines parallel to the wall, thus there is no visual indication of any swirling in the flow. However, a different picture is revealed by a hypothetical experiment.

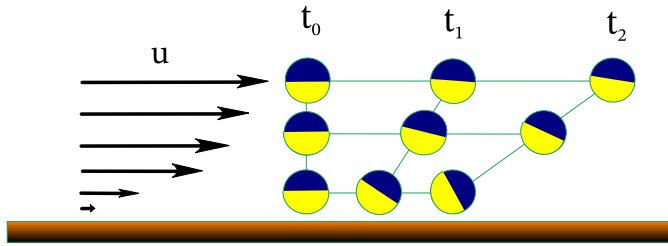

FIGURE 7.3 Wall generated vorticity

Let us insert a set of "vorticity markers" at various distances from the wall. The markers have a circular shape with the bottom and top halves painted by a light and dark color, respectively. This makes any rotation about the axis through the center of the markers easy to detect. At $t = t_0$, the markers have their color dividing diameter in the horizontal position. At the wall, the no-slip condition requires the velocity to vanish. Near the wall the velocity is smaller than that of the free stream, thus a velocity gradient is created, and the top side of a marker moves faster than the bottom, resulting in a clockwise rotation. The rotation is more pronounced near the wall where the velocity gradient assumes its highest value. Notice that the overall rotation of the markers increases from time t_1 to t_2 indicating that the vorticity is sustained over time.

There is evidence that vorticity is actually generated at a no-slip wall. Unfortunately, the fact that the velocity vanishes at the wall makes the visualization of vorticity close to a solid boundary difficult because a fluid element there cannot rotate as a whole. Thus, it is wise to simultaneously consider the strain rate of the fluid element, as it is skewed with one side attached to the wall.

Example 7.2.1. Let us compute the vorticity for the viscous flow driven by a moving plate that was described in section 5.11.1. Recall that the velocity profile is linear, and that the flow is contained in the $x - y$ plane. Therefore

$$\boldsymbol{\omega} = \left(\frac{\partial w}{\partial y} - \frac{\partial v}{\partial z}\right)\mathbf{i} + \left(\frac{\partial u}{\partial z} - \frac{\partial w}{\partial x}\right)\mathbf{j} + \left(\frac{\partial v}{\partial x} - \frac{\partial u}{\partial y}\right)\mathbf{k} = -\frac{U}{B}\mathbf{k} \qquad (7.4)$$

Hence, the vorticity vector is perpendicular to the plane of flow, and the rotation has a clockwise direction.

7.2.1 Horse-Shoe Vortex

The pattern of vortex lines and tubes becomes further complicated in three-dimensional shear flows where the axis of rotation changes orientation arbitrarily, as shown in Fig. 7.4.

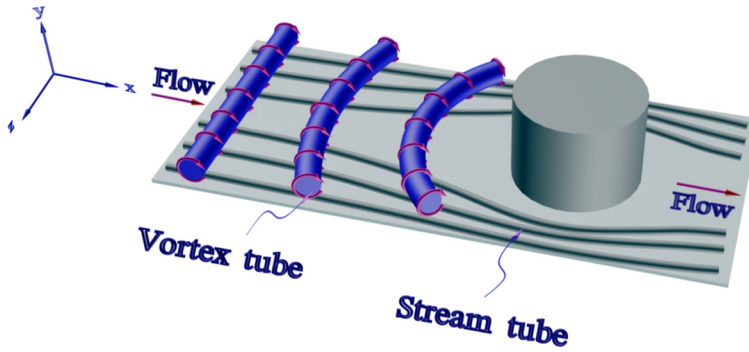

FIGURE 7.4 Vortex tube in shear flow around a cylinder

The example shown corresponds to a shallow stream approaching a cylindrical bridge pier. For simplicity, the stream bed is assumed horizontal. The flow is oriented along the x axis, and is assumed uniform in the transverse, z, direction far upstream of the pier. The no-slip condition at the bottom of the stream forces fluid elements to rotate clockwise, and we can imagine a straight vortex tube forming across the stream upstream of the pier.

As the flow approaches the pier, the stream tubes bend in order for the fluid to pass around the pier, and at the same time the vortex tubes bend and twist, as the plane of rotation constantly changes with position. Further downstream, the vortex pattern becomes very complicated, thus it is not easy to predict it without careful experiments or a numerical simulation of the flow. The vortex formation shown in Fig. 7.4 is an important phenomenon that has major implications on the wind loading of tall buildings, and the erosion of the channel bed in the vicinity of bridge piers. The shape of the vortex is similar to a horse shoe around the object when looked at from above, thus the name *horse-shoe vortex*.

7.2.2 Vorticity in Natural Coordinates

The presence of vorticity in shear flow is difficult to distinguish from the more obvious vorticity generated by a generally swirling flow. It is therefore advantageous to re-examine the concept of vorticity in natural coordinates, especially in two-dimensional flow applications where it is easier to visualize the normal and tangential velocity components. In these cases, vorticity can also be expressed in natural coordinates, which allows an alternative physical interpretation of the vorticity components.

Let us recall the approach for estimating the radius of curvature at some point P on a streamline, as described in section 2.8.4. By similar arguments we can also estimate the tangential and normal derivatives of the velocity at point P in terms of the Cartesian components of the velocity, u and v. Referring to Fig. 7.5, consider the streamline through point P. For simplicity, we have taken the x axis to coincide with the tangent to the streamline at P, thus $u = V = |\mathbf{V}|$ and

$$\frac{\partial u}{\partial y} = \frac{\partial V}{\partial n} \tag{7.5}$$

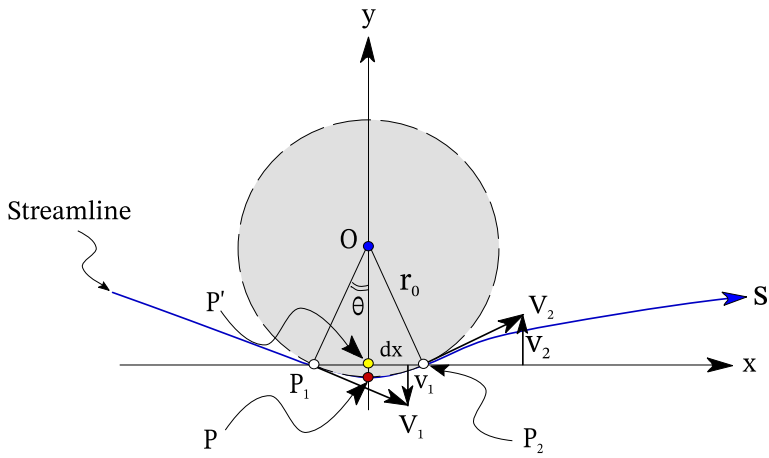

FIGURE 7.5 Vorticity in natural coordinates

where n is the direction normal to the streamline. The derivative of the normal component of the velocity can be computed by considering two points, P_1 and P_2, at a distance dx on each side of P. Therefore, the normal velocity components at these points are $v_2 = V \sin\theta$, and $v_1 = -V \sin\theta$, respectively. As the angle θ approaches zero, the x derivative of v at P can then be approximated by the following expression

$$\frac{\partial v}{\partial x} = \frac{v_2 - v_1}{2dx} = \frac{2V \sin\theta}{2r_0 \sin\theta} = \frac{V}{r_0} \tag{7.6}$$

Therefore, in natural coordinates in two space dimensions, the vorticity can be expressed by substituting Eqs. (7.5) and (7.6) in Eq. (5.86), as follows

$$\boldsymbol{\omega} = \left(\frac{V}{r_0} - \frac{\partial V}{\partial n}\right)\mathbf{k} \tag{7.7}$$

Eq. (7.7) allows us to separate the components of vorticity, and attach a physical interpretation to the causes of rotation in fluid motion. The first term is called

curvature vorticity, as it achieves its highest values during fast rotation around a small fluid cell. As the streamlines are flattened and the radius of curvature increases, curvature vorticity is diminished. The second term in Eq. (7.7) is called *shear vorticity*. It indicates the change in velocity across the streamlines that causes shearing of fluid layers. Clearly, the two components of vorticity may combine to produce the effects of local spin of the fluid.

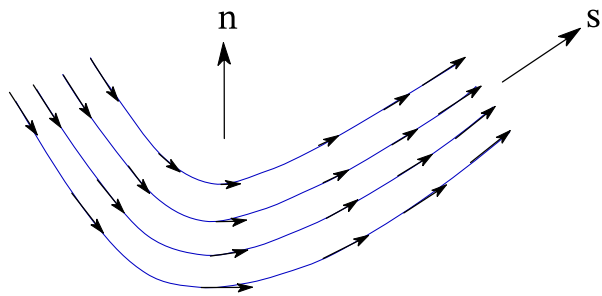

FIGURE 7.6 Vorticity in a current

Consider, for example, the stream shown in Fig. 7.6. As the stream goes around the bend, there is clearly an increase of velocity towards the outside of the bend. By definition, $V > 0$, and r_0 is also positive due to the definition for the sign of curvature in counterclockwise motion, as described in section 2.8.1. Therefore, the curvature vorticity is positive. The same is true for the shear vorticity since $-\frac{\partial V}{\partial n} > 0$, thus the total vorticity is maximized. The opposite would be true in clockwise rotation, thus the two vorticity terms may combine or cancel each other, depending on the flow orientation.

7.2.3 Circulation

Closely related to vorticity is the concept of circulation, Γ, defined as the amount of fluid rotation within a closed path. Thus, while vorticity is a local measure of the swirling of the flow that is unique at every point, circulation is a macroscopic measure of fluid rotation over a finite region. Specifically

$$\Gamma = \oint_L \mathbf{V} \cdot \mathbf{t}\, dL \tag{7.8}$$

in which L is a closed curve and $\mathbf{t}$ is the unit vector tangent to L at every point. Eq. (7.8) defines the circulation as the line integral of the tangential component of velocity taken around a closed curve in space. For example, the line integral around the perimeter of the entrance and exit faces of the stream tube in Fig. 2.14 determines the circulation at those sections, thus its value is called the *strength of the vortex tube*.

7.2.4 Divergence of the Vorticity Field

Vorticity is intimately connected to the concept of circulation and some important theorems of fluid mechanics will be presented in section 7.7. Presently, it is important to point out that the curl and divergence of the velocity field combine through the vector identity proven in section 2.2.7. It follows that

$$\nabla \cdot \boldsymbol{\omega} = \nabla \cdot \nabla \times \mathbf{V} = 0 \tag{7.9}$$

Notice the similarity with Eq. (5.11). The vorticity field is by definition divergence-free or *solenoidal* while this is only true for the velocity field in the case of incompressible flow. Recall also that a conservative vector field is one whose curl vanishes identically, according to Eq. (2.32). Furthermore, a conservative vector field can always be expressed as the gradient of some scalar field. Solenoidal vector fields have a similar physical interpretation, as they can be expressed as the curl of another vector field, sometimes called the *vector potential*. Thus, Eq. (7.9) is an important vector relation in fluid mechanics because it holds true for *all* vorticity fields.

7.3 VORTEX SHEETS

Observations of flow fields indicate that vorticity is concentrated in regions where the velocity field undergoes sudden changes. The connection is not immediately obvious, thus it is important to examine what happens to the velocity in the presence of vortices. Let us consider a planar array of vortex filaments that forms a flat, isolated *vortex sheet*, as shown in Fig. 7.7.

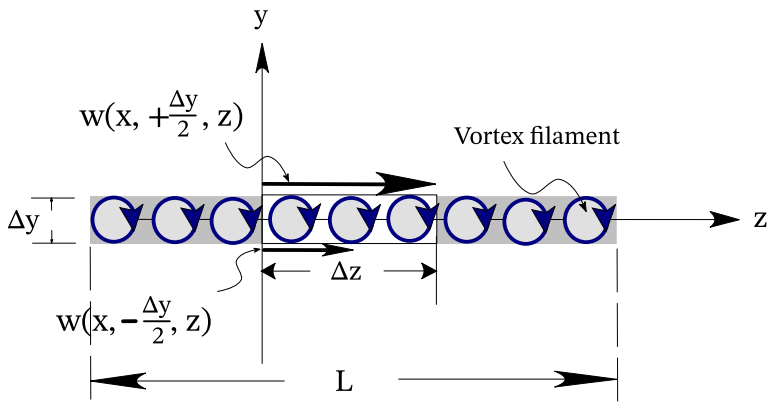

FIGURE 7.7 Vortex sheet

The easiest way to explain a vortex sheet is to imagine a single vortex of strength Γ being repeatedly subdivided into smaller vortices distributed along a line of length L. As the size of the vortices approaches zero, the line becomes a vortex sheet whose vortex strength is uniformly spread over the length L, i.e.

$$\gamma_x = \frac{\Gamma}{L} \tag{7.10}$$

where γ_x is the intensity of the sheet per unit length. The subscript x indicates that the vortex filaments are oriented along the x axis. The dimensions of γ_x are similar to velocity, i.e. L/T. In Fig. 7.7, we have assumed that the flow is aligned with the z axis, thus the only non-zero component of velocity is w, and the vortex sheet in the figure lies entirely on the $x - z$ plane.

The strength of the vortex sheet is found by integration of the tangential velocity around an elementary rectangle with sides Δy, Δz, and embedded in the vortex sheet, as follows

$$d\Gamma = w\big|_{y=+\Delta y/2}\, dz - w\big|_{y=-\Delta y/2}\, dz$$

or

$$\gamma_x = \frac{d\Gamma}{dz} = \Delta w \tag{7.11}$$

Therefore, the intensity of the vortex sheet, per unit length, is equal to the velocity difference across the sheet, which suggests that the velocity tangent to the sheet experiences a discontinuity as we move from one to the other side of the sheet. This is a result of importance in environmental flows because it proves the generation on vorticity at the interface between two parallel streams with different velocities. These are encountered in jets and mixing layers, and are associated with the spreading of pollutants.

For an arbitrarily oriented vortex sheet, the vortex intensity becomes a vector with components $(\gamma_x, \gamma_y, \gamma_z)$ that can be generally written as follows

$$\boldsymbol{\gamma} = \mathbf{n} \times \Delta \mathbf{V} \tag{7.12}$$

where $\mathbf{n}$ is the unit vector normal to the vortex sheet. As a result, vortex sheets can take very complex forms in areas of intense swirling in the flow field, acquiring multiple folds and bends.

In retrospect, it is tempting to conclude that the curvilinear wall of a vortex tube shown in Fig. 7.1 can be generated by rolling up a vortex sheet to form a closed loop, as was the case with the stream tube discussed in section 2.6.1. However, for viscous fluids, the boundary of a vortex tube is not sharply defined because a vortex tube actually consists of a viscous core surrounded by a diffused vortex sheet. This is manifested easily by a simple experiment. If we rotate a solid rod about its axis inside a fluid container, the no-slip condition will help transfer the angular momentum of the rod to the fluid. The vorticity will then gradually spread to the rest of the fluid not by a finite speed, but diffusing like solute mass or heat. This makes the dynamics of a vortex one of the most interesting and complicated subjects of fluid mechanics, as it forms the basis for understanding the effects of viscosity near solid boundaries. Drag and lift are also given additional physical clarity, as it will be further discussed in the following sections.

7.3.1 Stream Induced by Vorticity

While it makes physical sense to consider the creation of vorticity as a result of changes in the velocity field, it is also possible to think that vorticity itself can induce motion of fluid particles, and therefore generate a stream. The idea is common in electromagnetism where a steady current is connected to the surrounding magnetic field. The process is governed by the *Biot-Savart law*, named after Jean-Baptiste Biot and Félix Savart, who discovered this relationship in 1820.

The law states that "the magnetic field decreases with the square of the distance from a current element." By analogy, a vortex element $d\mathbf{l}$ centered at point P "induces" an elemental velocity $d\mathbf{V}$ at a point P', as follows

$$d\mathbf{V} = \frac{\Gamma}{4\pi} \frac{d\mathbf{l} \times \mathbf{r}}{r^3} \tag{7.13}$$

where r is the magnitude of the vector $\mathbf{r}$ connecting the points P and P', as shown in Fig. 7.8. Notice that the notion of "induced" velocity is not exactly correct in fluid flow, because no causality can be established between vorticity and velocity, as is the case for current and magnetic field. However, the Biot-Savart law still provides an inversion of vorticity method of physical significance.

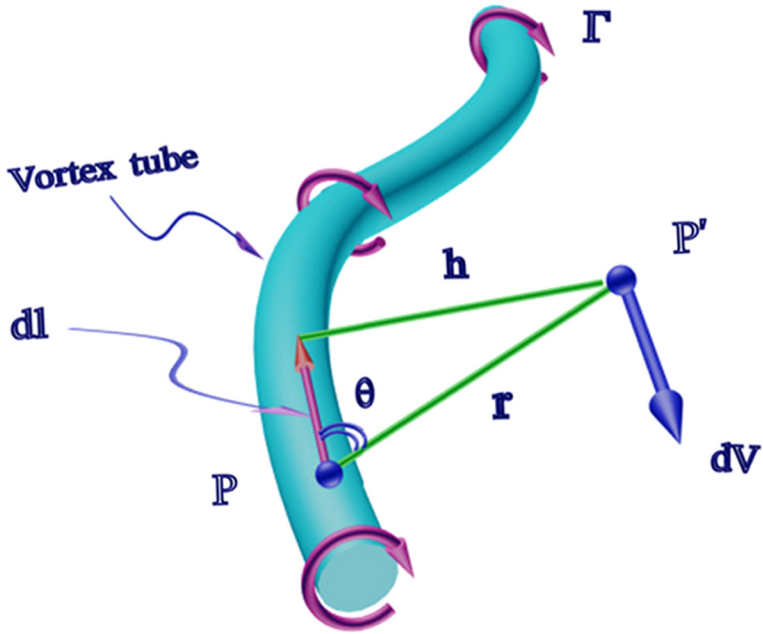

FIGURE 7.8 Vorticity induced velocity

If the vortex tube is straight and of infinite length, the velocity at point P can be found by integration of Eq. (7.13), as follows

$$\mathbf{V} = \frac{\Gamma}{4\pi}\int_{-\infty}^{\infty}\frac{d\mathbf{l}\times\mathbf{r}}{r^3} = \frac{\Gamma}{4\pi}\int_{-\infty}^{\infty}\frac{1}{r^2}\sin\theta\, dl \tag{7.14}$$

Referring to Fig. 7.8, $r = h/\sin\theta$ and $dl = hd\theta/\sin^2\theta$, where h is the perpendicular distance of point P from the vortex segment $d\mathbf{l}$. Then, Eq. (7.14) can be rewritten as follows

$$\mathbf{V} = \frac{\Gamma}{4\pi h}\int_0^{\pi}\sin\theta d\theta = \frac{\Gamma}{2\pi h} \tag{7.15}$$

In general, $\Gamma d\mathbf{l} = \boldsymbol{\omega} d\mathcal{V}$. Then, invoking *Stokes' circulation theorem* (cf. section 7.7), we can write the Biot-Savart law in terms of the vorticity, i.e.

$$\mathbf{V} = \frac{\Gamma}{4\pi}\int_{\mathcal{V}}\frac{\boldsymbol{\omega}\times\mathbf{r}}{r^3}\, d\mathcal{V} \tag{7.16}$$

The physical implications of Eq. (7.16) are significant in environmental fluid mechanics. The most important rule dictates that the vorticity may not be prescribed arbitrarily in a flow domain, but instead must satisfy Eq. (7.16). Thus, when we speak of "vorticity generation" at a solid boundary in steady flow, we may not conclude that the process is somehow independent of the existing velocity field.

7.4 CONCENTRATED VORTICES

Although in the preceding sections we have used the term vortex casually, a formal definition of a vortex is difficult. A vortex tube surrounded by irrotational flow is one option, but we must concede that the vortex wall becomes diffused as viscosity increases. Another option is to think of a *vortex core*, and then an outer boundary where the circumferential velocity reaches a maximum value. There are some clear examples of isolated vortices in environmental flows, however, that are of practical importance.

7.4.1 The Forced Vortex

Rigid body rotation occurs when a fluid is rotated without relative motion of fluid particles. This is the case, for example, of a fluid placed in a cylindrical container on top of a turntable rotating with a constant angular velocity, Ω_0. After some time elapses, a steady state is achieved, in which the tangential velocity varies linearly with radial distance, r, while both the radial and axial components of the velocity vector vanish, i.e.

$$v_\theta = r\Omega_0 \qquad v_r = 0 \qquad v_z = 0 \tag{7.17}$$

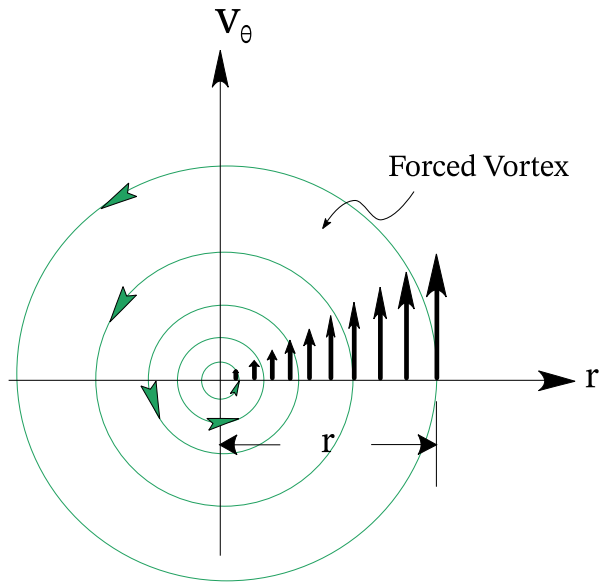

FIGURE 7.9 Forced vortex

As shown in Fig. 7.9, the simplicity afforded by the cylindrical coordinate system should be obvious. The vorticity of the flow field can be calculated from

Eq. (7.3), as follows

$$\omega_z = \frac{1}{r}\frac{\partial}{\partial r}\left(r^2\Omega_0\right) = 2\Omega_0 \tag{7.18}$$

Notice that the vorticity is constant and equal to twice the angular velocity, complying perfectly with the expectation for a rigid body rotation. Similarly, the circulation is computed from Eq. (7.8), as follows

$$\Gamma = \oint_0^{2\pi} v_\theta r\, d\theta = 2\pi r^2\Omega_0 \tag{7.19}$$

Notice that the circulation is equal to the vorticity times the cross-sectional area of the container holding the fluid. This type of rotational flow is often called a *forced vortex* to emphasize the fact that the rotation is induced externally, and that the fluid essentially rotates as a rigid body.

It is a common observation that, if the fluid that is subjected to forced rotation has a free surface, a depression is created around the axis of rotation, z. This is due to the pressure gradient in the r direction that is necessary to balance the centrifugal force. Thus, summing forces along the radial direction, we can write

$$\frac{1}{\rho}\frac{\partial p}{\partial r} = \frac{V_\theta^2}{r} \tag{7.20}$$

In the vertical direction, the pressure gradient is simply balanced by gravity, i.e. the pressure variation is hydrostatic

$$\frac{1}{\rho}\frac{\partial p}{\partial z} = -g \tag{7.21}$$

Therefore, the total differential of the pressure can be found by combining Eqs. (7.20) and (7.21), as follows

$$\begin{aligned} dp &= \frac{\partial p}{\partial r}dr + \frac{\partial p}{\partial z}dz \\ &= \rho\left(\frac{V_\theta^2}{r}dr - g dz\right) \\ &= \rho\left(\Omega^2 r dr - g dz\right) \end{aligned} \tag{7.22}$$

Then, setting dp equal to zero, we obtain a relation describing surfaces of constant pressure. To find the shape of the free surface, Eq. (7.22) can be rearranged to represent the variation of the *piezometric head*, as follows

$$d\left(\frac{p}{\rho g} + z\right) = \frac{1}{g}\Omega^2 r dr \tag{7.23}$$

The piezometric head is equal to the depth, h, measured from the bottom of the container, thus following integration of Eq. (7.23), we obtain the shape of the free surface, i.e.

$$h = h_0 + \frac{\Omega^2 r^2}{2g} \tag{7.24}$$

where h_0 is the depth at the center of the vortex. As shown in Fig. 7.10, the shape of the free surface is a paraboloid of revolution, which agrees well with observations. Notice that the forced vortex exists essentially under hydrostatic conditions, and there is no relative motion of fluid particles.

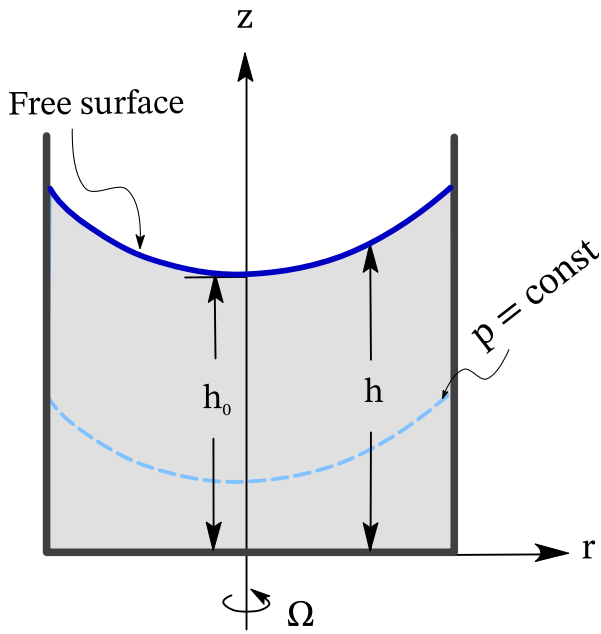

FIGURE 7.10 Pressure in forced vortex

7.4.2 The Free (Irrotational) Vortex

Another simple rotational flow pattern that is often encountered in environmental flows occurs when the effects of viscosity can be neglected. In such cases, a steady-state flow field is established that is characterized by circular streamlines and a tangential velocity that decreases with distance, r, from the center of rotation. This is the well-known *sink vortex* encountered when a reservoir is emptied from a small bottom orifice.

The flow pattern of the sink vortex can be approximated by a simple model using cylindrical coordinates, as shown in Fig. 7.11A. Let us assume the velocity

has the following components

$$v_\theta = \frac{C}{r} \qquad v_r = 0 \qquad v_z = 0 \tag{7.25}$$

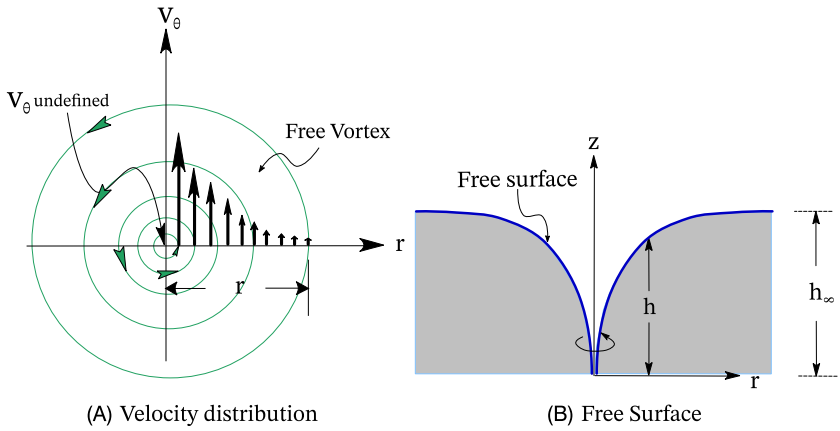

FIGURE 7.11 Irrotational (free) vortex

where the constant C is called the *strength of the vortex*. The associated flow pattern is known as a *free vortex*, and its vorticity is given by

$$\omega_z = \frac{1}{r}\frac{\partial}{\partial r}(C) = 0 \tag{7.26}$$

Therefore, although the fluid is visually undergoing a swirling motion, the flow is strictly irrotational. Notice that Eq. (7.25) is not valid at $r = 0$ where both the velocity and vorticity fields are not defined. The circulation on the other hand is given by

$$\Gamma = \oint_0^{2\pi} v_\theta r \, d\theta = 2\pi C \tag{7.27}$$

which is constant and independent of the radial distance. It can be seen that the vortex strength, C, has dimensions of L^2/T, and represents the circulation per unit length measured around a circle of unit radius, i.e. $C = \Gamma/2\pi$. Since the circulation is directly related to the vorticity through Eq. (7.8), $\boldsymbol{\omega}$ must be non-zero somewhere in the domain. Since $\boldsymbol{\omega}$ is undefined at the center of rotation, we conclude that $\boldsymbol{\omega} \to \infty$, at $r = 0$. This singularity at the center of rotation in a free vortex can also be seen in the following computational example, in which the origin is avoided when using a Cartesian mesh to discretize a free vortex on the $x - y$ plane.

The pressure variation and the shape of the free surface of the free vortex can be found once again by computing the total differential of the pressure.

Substituting of Eq. (7.25) in Eq. (7.22) yields

$$dp = \rho \frac{C^2}{r^3} dr - \rho g dz \tag{7.28}$$

Thus, the pressure variation has a singularity at $r = 0$. On the other hand, as $r \to \infty$, the pressure distribution becomes hydrostatic. We therefore expect the free surface to be horizontal at infinity, and decrease sharply as the center of rotation is approached, as shown in Fig. 7.11B. Similar to the case of the forced vortex, we can express the depth from an arbitrary datum in terms of the piezometric head. Then, following integrating, we obtain

$$\int_h^{h_\infty} dh = C^2 \int_0^\infty \frac{dr}{g r^3} \tag{7.29}$$

Therefore

$$h = h_\infty - \frac{C^2}{2 g r^2} \tag{7.30}$$

where h_∞ is the depth at infinity. In practice, the pressure and the free surface elevation do not go to $-\infty$ due to interference of solid boundaries with the vortex. Thus, the singularity as $r \to 0$ is avoided. Nevertheless, very low values of pressure are generated in so-called super cells in the atmosphere leading to the formation of tornados.

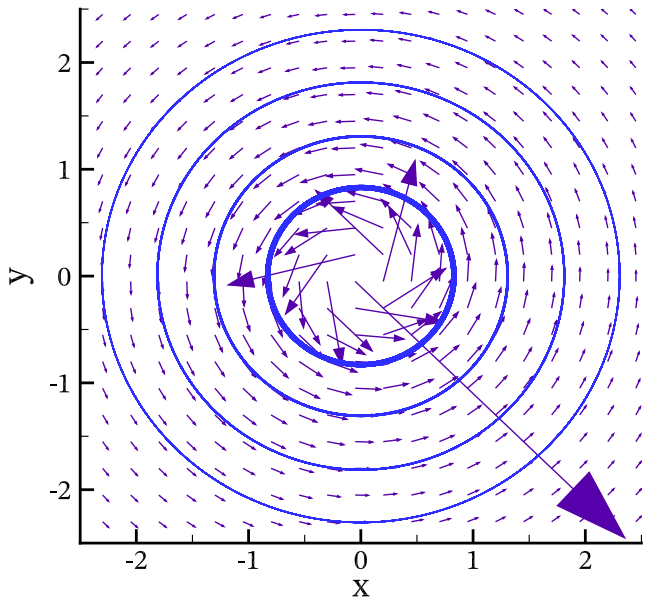

FIGURE 7.12 Irrotational vortex

Example 7.4.1. Let us consider the velocity field shown in Fig. 7.12. The flow is two-dimensional and the velocity vector field is described by

$$\mathbf{V} = -\frac{y}{x^2+y^2}\mathbf{i} + \frac{x}{x^2+y^2}\mathbf{j} + 0\mathbf{k}$$

Therefore the rotation vector is aligned with the z axis, i.e. the rotation is limited to the $x-y$ plane. As we attempt to compute the velocity field, it becomes apparent that the velocity is not defined at $x=0$, $y=0$. Actually, if the origin is included in the calculations, the field is rotational. If, however, we exclude the z-axis, a simple computation shows that the field becomes irrotational, as the curl vanishes everywhere else. This observation leads to the idea of a combined vortex model, in which the center area of rotation is replaced by a simple rotational flow pattern, as shown in the next section.

7.4.3 The Rankine Vortex

A simple yet excellent model for a real hurricane is given by the *Rankine vortex*, named after William John Macquorn Rankine (1820–1872), who was a Scottish civil engineer, physicist, and mathematician. He made significant contributions to thermodynamics and fluid mechanics, as well as to the theory of frames and retaining walls. The Rankine vortex combines a rigid core inner vortex with an irrotational vortex in the far field, as follows

$$v_\theta = \begin{cases} \Omega_0 r, & \text{if } r \le R \\ \frac{C}{r}, & \text{if } r > R \end{cases} \qquad v_r = 0 \qquad v_z = 0 \tag{7.31}$$

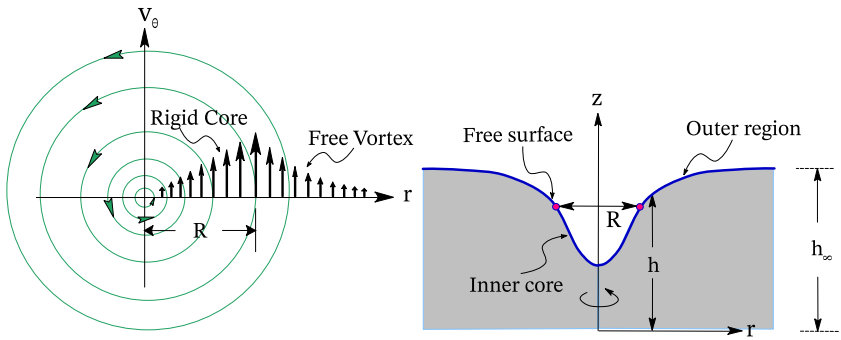

(A) Velocity distribution (B) Free Surface

FIGURE 7.13 Rankine combined vortex

The inner part of the flow, i.e. the region characterized by a radial distance $r \le R$, corresponds to a rigidly rotating core while the outer region becomes a free vortex, as shown in Fig. 7.13A. This prevents the velocity from becoming

infinite at the center of rotation. At the same time, for a radial distance $r > R$, the model reverts to a free vortex, which allows for the velocity to decay at large distances, as physical observations of real hurricanes suggest. Using Eq. (7.3), the vorticity of the flow can be written as follows

$$\omega_z = \frac{v_\theta}{r} + \frac{\partial v_\theta}{\partial r} = \begin{cases} 2\Omega_0, & \text{if } r \leq R \\ 0, & \text{if } r > R \end{cases} \tag{7.32}$$

As a result, the vorticity field is discontinuous at $r = R$ while the velocity field only has a slope discontinuity at that point. At the edge of the inner core, i.e. at $r = R$, the circulation is given by Eq. (7.19). The inner core circulation must also be equal to the value of Γ at $r = R$, as computed in the outer region by Eq. (7.27). Thus, the strength of the free vortex can be related to the inner core rotation, as follows

$$C = R^2 \Omega_0 \tag{7.33}$$

The strength of the free vortex can be identified independently, if measurements of the tangential velocity are made in the outer region of the vortex. For example, the three major parameters of the model, i.e. C, R, and Ω_0, can be identified if in addition an estimate of the maximum velocity, at $r = R$, is available.

The pressure variation in the Rankine vortex can be again computed by a balance between the pressure gradient and the centrifugal force. The total differential of pressure in the inner core is given by Eq. (7.22), and by Eq. (7.28) in the outer region. Therefore, the rates of change of the piezometric head with radial distance for the core and outer regions are given by

$$\left.\frac{dh}{dr}\right|_{inner} = \frac{\Omega^2 r}{g} \qquad \text{and} \qquad \left.\frac{dh}{dr}\right|_{outer} = \frac{C^2}{g r^3} \tag{7.34}$$

Then, upon substitution of Eq. (7.33) and evaluation at $r = R$, we find that

$$\left.\frac{dh}{dr}\right|_{inner} = \left.\frac{dh}{dr}\right|_{outer} = \frac{C^2}{g R^3} \tag{7.35}$$

Thus, the free-surface is continuous at $r = R$, and the Rankine vortex has a smooth profile that combines those of the forced and free vortices, as shown in Fig. 7.13B. The inner core prevents the free surface from attaining an infinite slope at the center of rotation, while the outer region allows the vortex to approach hydrostatic conditions at infinity.

7.5 CELLULAR FLOWS

In a variety of environmental flows, it is common to find fluid motions that have a cellular character, in which the flow forms closed loops in the form of a cell. An example is the Rayleigh-Bérnard convection that occurs for very small temperature gradients in a shallow layer of fluid contained between two parallel plates while the bottom plate is heated uniformly from below (Rayleigh, 1916, Bénard, 1900).

This is an important phenomenon that affects local climate, building ventilation and many industrial processes. Bénard was the first to observe the onset of convective motion at a critical value of heating of the bottom plate. Fluid appeared to rise in a cyclic motion forming a two-dimensional rolling motion. The solution of this problem is complicated, as it requires coupling of the energy and Navier-Stokes equations.

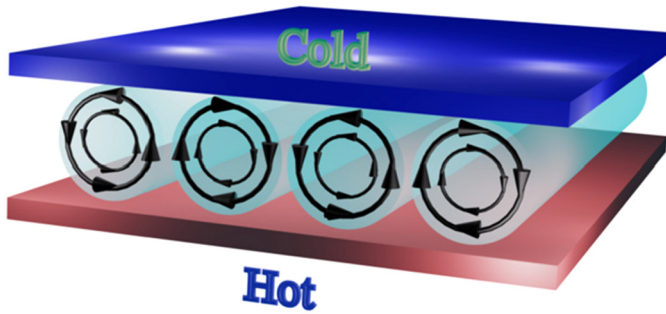

FIGURE 7.14 Cellular velocity field

Lord Rayleigh proposed an analytical model for Bénard's thermal convection problem based on the buoyancy of the heated fluid. A schematic of the system studied by Rayleigh is shown in Fig. 7.14. The cold fluid near the top plate is denser than the hot fluid near the bottom plate. As the thermal gradient increases, the buoyancy of the fluid creates an overturning instability, leading to convection rolls. For relatively smaller thermal gradients, buoyancy is counteracted by the viscous dissipation and conduction of heat, thus the rolls remain stable. In this simple model, the flow is purely two-dimensional and is characterized by a series of cells rotating in such a way as to create down and upwelling of the fluid. The analytical solution requires some further assumptions that are presented in Chapter 10. However, a simple example of cellular flow can be constructed for present purposes by introducing a two-dimensional flow pattern that has a similar velocity field, as follows

$$\mathbf{V} = \sin \pi x \cos \pi y \mathbf{i} - \cos \pi x \sin \pi y \mathbf{j} \tag{7.36}$$

Notice that the flow is contained in the $x - y$ (vertical) plane, as there is no component of flow parallel to the plates, i.e. the z direction. This velocity field

provides an excellent opportunity for studying the vorticity and fluid deformation in cellular flows, as the velocity pattern resembles that of the Rayleigh-Bérnard convection. Furthermore, by computing the divergence of Eq. (7.36) it is easy to show that the velocity field is solenoidal, i.e. the flow satisfies the incompressibility constraint given by Eq. (5.11).

The velocity field corresponding to Eq. (7.36) is shown in Fig. 7.16 for a group of four cells. The vorticity is computed using Eq. (5.86), as follows

$$\boldsymbol{\omega} = 2\pi \sin \pi x \sin \pi y \mathbf{k} \tag{7.37}$$

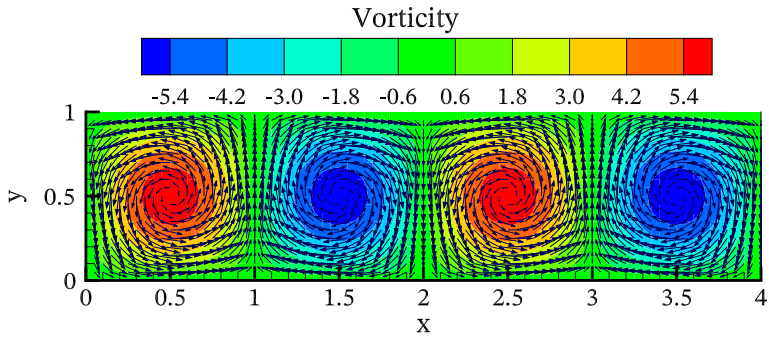

FIGURE 7.15 Cellular velocity field

Therefore, the vorticity vector is pointing in the $\pm z$ direction matching the cell dynamics of Rayleigh-Bérnard convection. As shown in Fig. 7.15, the vorticity reaches its maximum magnitude at the cell centers while the vorticity direction alternates between neighboring cells. As a result, the vorticity vanishes at the cell borders creating a layer of zero rotation around each cell.

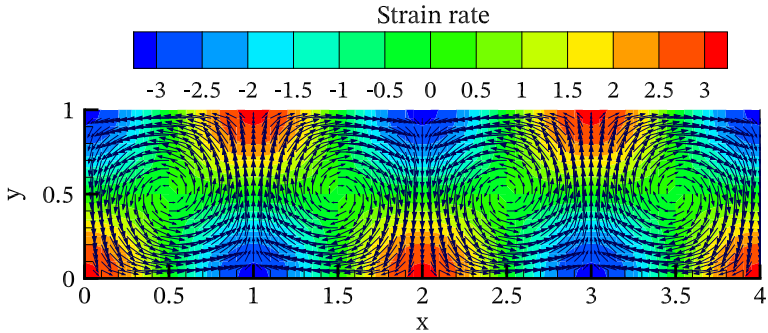

FIGURE 7.16 Cellular velocity field

The rate-of-strain of the velocity field can be computed using Eq. (5.71), as follows

$$S_{ij} = \begin{pmatrix} \pi \cos \pi x \cos \pi y & 0 \\ 0 & -\pi \cos \pi x \cos \pi y \end{pmatrix} \tag{7.38}$$

As shown in Fig. 7.16, the rate-of-strain vanishes at the cell centers. Furthermore, the rate-of-strain achieves its maximum magnitude at the cell corners. Notice, however, that the sign of S_{ij} alternates from corner to corner, thus the rate-of-strain vanishes at the mid point of each edge. Finally, contraction of S_{ij} confirms once again the incompressibility of the flow.

The behavior of cellular flow has significant implications for environmental applications, such mass transport, as both the vorticity and rate-of-strain have an effect on diffusion of solute mass, as it was shown in Chapter 3. Quenching of reactions may also occur in cellular flow depending on the relative length scales of the cell and the reaction (Fannjiang et al., 2006). In some cases, the thin boundary layer which forms along the boundaries of the cells has a profound effect on chemical reactions leading to some complicated diffusion-reaction phenomena.

7.6 THE VORTICITY TRANSPORT EQUATION

The concept of vorticity allows additional light to be shed on the equations of fluid motion, thus it has become customary to express the equations of flow in terms of the vorticity. This is usually accomplished by taking the curl of the momentum equation, i.e. Eq. (5.113), as follows

$$\boldsymbol{\nabla} \times \left[\frac{\partial \mathbf{V}}{\partial t} + (\mathbf{V} \cdot \boldsymbol{\nabla}) \mathbf{V} \right] = \boldsymbol{\nabla} \times \mathbf{g} - \boldsymbol{\nabla} \times \left(\frac{1}{\rho} \boldsymbol{\nabla} p \right) + \boldsymbol{\nabla} \times \left(\nu \boldsymbol{\nabla}^2 \mathbf{V} \right) \tag{7.39}$$

The evaluation of the vector products in Eq. (7.39) involves several important conceptual decisions, therefore we examine each term separately. First, the temporal derivative of the velocity yields

$$\boldsymbol{\nabla} \times \frac{\partial \mathbf{V}}{\partial t} = \frac{\partial \boldsymbol{\omega}}{\partial t} \tag{7.40}$$

Before evaluating the curl of the convective acceleration in Eq. (7.39), let us recall the triple vector product identity, i.e. Eq. (1.132). For present purposes, it can be written as follows

$$\mathbf{V} \times (\boldsymbol{\nabla} \times \mathbf{V}) = \boldsymbol{\nabla} (\mathbf{V} \cdot \mathbf{V}) - (\mathbf{V} \cdot \boldsymbol{\nabla}) \mathbf{V} \tag{7.41}$$

Then, following rearrangement and taking the curl, we obtain

$$\boldsymbol{\nabla} \times (\mathbf{V} \cdot \boldsymbol{\nabla}) \mathbf{V} = \boldsymbol{\nabla} \times \boldsymbol{\nabla} (\mathbf{V} \cdot \mathbf{V}) - \boldsymbol{\nabla} \times (\mathbf{V} \times \boldsymbol{\omega}) \tag{7.42}$$

Notice that $\mathbf{V} \cdot \mathbf{V}$ is a scalar, thus the first term on the right hand side vanishes because of Eq. (2.32). The second term on the right is the curl of a vector product that can be expanded using the identity (2.26), as follows

$$\boldsymbol{\nabla} \times (\mathbf{V} \times \boldsymbol{\omega}) = \mathbf{V} (\boldsymbol{\nabla} \cdot \boldsymbol{\omega}) + (\boldsymbol{\omega} \cdot \boldsymbol{\nabla}) \mathbf{V} - \boldsymbol{\omega} (\boldsymbol{\nabla} \cdot \mathbf{V}) - (\mathbf{V} \cdot \boldsymbol{\nabla}) \boldsymbol{\omega} \tag{7.43}$$

Notice that the first term on the right vanishes as a result of Eq. (7.9), which states that all vorticity fields are solenoidal, thus the divergence of vorticity is identically zero. The third term on the right hand side can be evaluated using the continuity equation, i.e. Eq. (5.8), as follows

$$\begin{aligned} \boldsymbol{\omega} (\boldsymbol{\nabla} \cdot \mathbf{V}) &= -\frac{\boldsymbol{\omega}}{\rho} \frac{D\rho}{Dt} \\ &= \rho \boldsymbol{\omega} \frac{D}{Dt} \left(\frac{1}{\rho} \right) \end{aligned} \tag{7.44}$$

Using Eqs. (7.40), (7.43), and (7.44), we can now write the curl of the inertia terms in Eq. (7.39) as follows

$$\begin{aligned}\frac{\partial \boldsymbol{\omega}}{\partial t} + (\mathbf{V}\cdot\boldsymbol{\nabla})\,\boldsymbol{\omega} + \rho\boldsymbol{\omega}\frac{D}{Dt}\left(\frac{1}{\rho}\right) - (\boldsymbol{\omega}\cdot\boldsymbol{\nabla})\,\mathbf{V} \\ = \frac{D\boldsymbol{\omega}}{Dt} + \rho\boldsymbol{\omega}\frac{D}{Dt}\left(\frac{1}{\rho}\right) - (\boldsymbol{\omega}\cdot\boldsymbol{\nabla})\,\mathbf{V} \\ = \rho\left[\frac{D\tilde{\boldsymbol{\omega}}}{Dt} - (\tilde{\boldsymbol{\omega}}\cdot\boldsymbol{\nabla})\,\mathbf{V}\right]\end{aligned} \tag{7.45}$$

where $\tilde{\boldsymbol{\omega}} = \boldsymbol{\omega}/\rho$ is the vorticity per unit mass.

Turning our attention to the right hand side of Eq. (7.39), we again recall from section 2.2.7 that the curl of the gradient of a scalar field is identically zero. Therefore, the curl of the gravitational force in Eq. (7.39) vanishes since the latter represents the gradient of the gravitational potential. The curl of the pressure gradient is also zero. However, since the density is variable, the pressure term does not vanish entirely. Specifically

$$\begin{aligned}\boldsymbol{\nabla}\times\left(\frac{1}{\rho}\boldsymbol{\nabla}p\right) &= \boldsymbol{\nabla}\left(\frac{1}{\rho}\right)\times\boldsymbol{\nabla}p \\ &= -\frac{1}{\rho^2}\left(\boldsymbol{\nabla}\rho\times\boldsymbol{\nabla}p\right)\end{aligned} \tag{7.46}$$

Finally, we focus on the viscous stresses. Observations of typical environmental flows show that although the density varies in space, the viscosity of the fluid remains approximately constant. By making this assumption, the computation of the curl of the viscous term in Eq. (7.39) is facilitated significantly because in this case we can write

$$\boldsymbol{\nabla}\times\left(\nu\boldsymbol{\nabla}^2\mathbf{V}\right) = \mu\boldsymbol{\nabla}\times\left\{\frac{1}{\rho}\left[\boldsymbol{\nabla}\left(\boldsymbol{\nabla}\cdot\mathbf{V}\right) - \boldsymbol{\nabla}\times\boldsymbol{\omega}\right]\right\} \tag{7.47}$$

where once again we made use of the triple vector product identity, i.e. Eq. (1.132). The divergence of the velocity on the right hand side can be eliminated using the continuity equation, as it was done in Eq. (7.44). Therefore, this term vanishes, as it is the curl of the gradient of a scalar. Then, expanding the vector product through the braces, we obtain

$$\begin{aligned}\boldsymbol{\nabla}\times\left(\nu\boldsymbol{\nabla}^2\mathbf{V}\right) &= -\mu\left[\frac{1}{\rho}\boldsymbol{\nabla}\times(\boldsymbol{\nabla}\times\boldsymbol{\omega}) + \boldsymbol{\nabla}\left(\frac{1}{\rho}\right)\times(\boldsymbol{\nabla}\times\boldsymbol{\omega})\right] \\ &= -\mu\left\{\frac{1}{\rho}\left[\boldsymbol{\nabla}\left(\boldsymbol{\nabla}\cdot\boldsymbol{\omega}\right) - \boldsymbol{\nabla}^2\boldsymbol{\omega}\right] + \boldsymbol{\nabla}\left(\frac{1}{\rho}\right)\times(\boldsymbol{\nabla}\times\boldsymbol{\omega})\right\}\end{aligned} \tag{7.48}$$

Again, the first term in the braces vanishes because the vorticity field is also solenoidal, as shown in Eq. (7.9). The second term in the braces represents the

viscous interaction between the density gradient and the curl of vorticity. This term may be significant near solid boundaries or where large curls of vorticity exist. Otherwise, the term may be neglected, as it is usually much smaller than the rest of the terms in the equation of vorticity transport. Therefore, substitution of Eqs. (7.45), (7.46), and (7.48) in Eq. (7.39) leads to the following equation

$$\frac{D\tilde{\boldsymbol{\omega}}}{Dt} = (\tilde{\boldsymbol{\omega}} \cdot \nabla)\,\mathbf{V} + \frac{1}{\rho^3}(\nabla\rho \times \nabla p) + \nu\nabla^2\tilde{\boldsymbol{\omega}} \tag{7.49}$$

This is the vorticity evolution equation for a compressible fluid. The material derivative on the left hand side of Eq. (7.49) represents temporal changes in vorticity that occur in the flow field as a result of pressure and viscous forces. The material derivative also shows that vorticity is advected by the velocity field, in a fashion very similar to the velocity vector in the Navier-Stokes equations.

The first term on the right hand side is new and requires some discussion. In a flow field, vortex tubes can be imagined superimposed on the velocity vector field. At a given point in space, there is one component of the velocity vector tangent to the vortex tube while the other two are perpendicular to the vortex tube. The latter components have the effect of tilting the axis of the vortex tube while variations of the former may stretch or contract the vortex tube in the direction of its axis. The stretching of a vortex tube is equivalent to reducing the radius of gyration around the vortex tube, thus increasing the vorticity. This action is known as *vortex stretching*, and is a result of the interplay between the vorticity $\boldsymbol{\omega}$ and the gradient of the velocity vector $\nabla\mathbf{V}$, which is a tensor representing the deformation of the fluid element. The result is a vector that

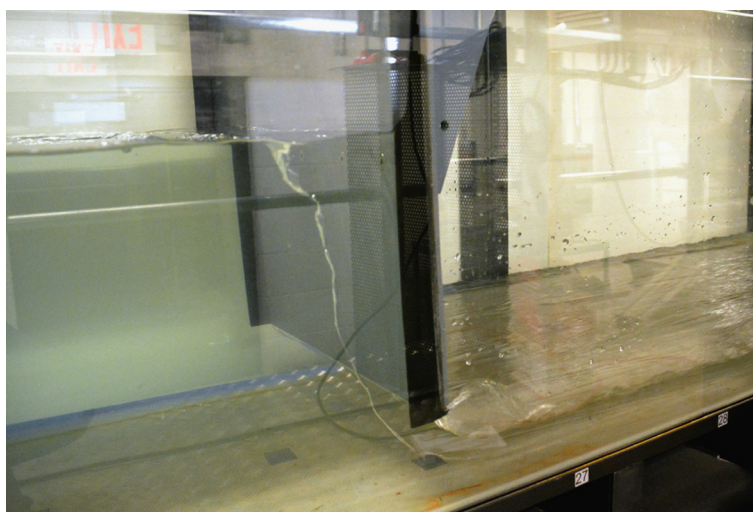

FIGURE 7.17 Vortex stretching under sluice gate

describes the stretching of vortex tubes associated with an increase in vorticity or the contraction of vortex tubes resulting in a decrease in vorticity.

Consider, for example, a vortex that is forced to dive under a sluice gate, as shown in Fig. 7.17. This type of vortex is produced as a result of the no-slip condition at the side walls of the channel. A short distance upstream of the gate, the vortex is vertical and has a uniform diameter. As it approaches the gate, however, the vortex is bent and stretched by the accelerating fluid. The intensity of the vorticity increases, and the vortex tube becomes aligned with the streamlines of the flow. Vortices are formed on both side walls of the channel. These vortices rotate in opposite directions due to the shear flow next to the walls. Upstream of the gate the vorticity vector points in the vertical direction due to rotation on the horizontal plane. In contrast, downstream of the gate the vorticity vector points in the stream-wise direction due to rotation on the vertical plane normal to the flow direction.

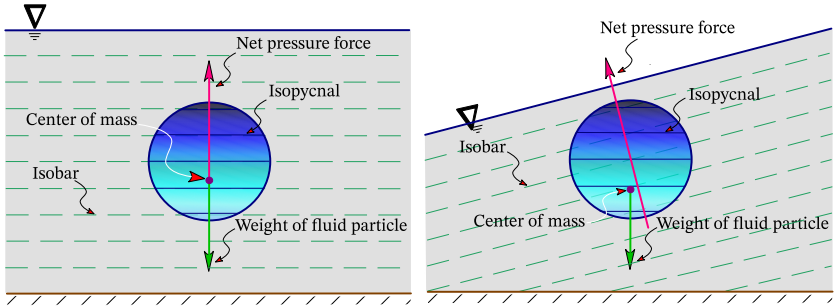

(A) Horizontal isobars (B) Tilted isobars

FIGURE 7.18 Net pressure and weight of fluid particle

The second term on the right hand side of Eq. (7.49) is also new, and represents the vector product between the gradients of the pressure and density fields. As shown in Fig. 7.18A, a fluid particle in a hydrostatic, density stratified flow, is subjected to a pressure force that is perpendicular to the isobars and passes through the geometric center of the particle. In this case, according to Eq. (1.20), $\nabla p = -\rho \mathbf{g}$, thus the isobars are parallel to the isopycnal lines, and the baroclinic term in Eq. (7.49) vanishes identically. However, if there is an inclination between the isobars and isopycnal lines, as shown in Fig. 7.18B, then the weight of the particle and the net pressure force are not aligned. This results in a torque $\nabla p \times \nabla \rho$ that tends to rotate the fluid particle, and vorticity is generated. This is known as the *baroclinic effect*. It requires that density variations be independent of pressure. For example, they could be the result of changes in temperature in the atmosphere or salinity in an estuary. Then, if the pressure gradient for some reason is inclined to the isopycnal lines, the net force on a fluid element does not pass through its center of mass, and vorticity is produced.

On the other hand, the second term in Eq. (7.49) vanishes for barotropic flows, i.e. when the density is a function of pressure only.

The third term on the right hand side of Eq. (7.49) represents the diffusion of vorticity by viscosity. Diffusion is a physical process that was discussed in detail in Chapter 3. Presently, it should suffice to say that this particular term of the vorticity equation tends to spread vortices away from a rough boundary, or other locations where vorticity is generated, to the rest of the flow due to non-zero gradients of the vorticity field. Diffusion also tends to attenuate the intensity of the vortices as they are spread away from their point of generation.

For an incompressible fluid, Eq. (7.49) can be further simplified because the divergence of the velocity vanishes, thus it no longer needs to be eliminated by means of the continuity equation. We can therefore drop the tildes from $\boldsymbol{\omega}$, and express the vorticity evolution as follows

$$\frac{D\boldsymbol{\omega}}{Dt} = (\boldsymbol{\omega} \cdot \boldsymbol{\nabla})\,\mathbf{V} + \frac{1}{\rho^2}(\boldsymbol{\nabla}\rho \times \boldsymbol{\nabla} p) + \nu \boldsymbol{\nabla}^2 \boldsymbol{\omega} \tag{7.50}$$

For completeness of the presentation and future use, it is useful to rewrite the vorticity transport equation in index form, i.e.

$$\frac{D\omega_i}{Dt} = \omega_j \frac{\partial u_i}{\partial x_j} + \frac{1}{\rho^2}\epsilon_{ijk}\frac{\partial \rho}{\partial x_j}\frac{\partial p}{\partial x_k} + \nu \frac{\partial^2 \omega_i}{\partial x_j \partial x_j} \tag{7.51}$$

Finally, for a barotropic flow, i.e. when the density is only a function of pressure, the baroclinic term may be neglected, leading to further simplification, as follows

$$\frac{D\boldsymbol{\omega}}{Dt} = (\boldsymbol{\omega} \cdot \boldsymbol{\nabla})\,\mathbf{V} + \nu \boldsymbol{\nabla}^2 \boldsymbol{\omega} \tag{7.52}$$

This is the simplest form of the vorticity transport equation for a viscous fluid. It is evident that the vorticity of a fluid parcel is not conserved, as the parcel moves with the fluid velocity. Instead the vortex is stretched, twisted and dispersed from the areas of vorticity generation.

7.6.1 Diffusion of Vorticity

It is interesting to examine the transport of vorticity in the case of the suddenly accelerated plate analyzed in section 5.11.4.1. Under the conditions of this problem, vortex stretching and tilting may be neglected, thus Eq. (7.52) can be further simplified, as follows

$$\frac{\partial \boldsymbol{\omega}_z}{\partial t} = \nu \frac{\partial^2 \boldsymbol{\omega}_z}{\partial y^2} \tag{7.53}$$

Thus the governing equation assumes the form of a pure diffusion equation for the vorticity. The initial and boundary conditions for this problem are as follows.

Initially, the vorticity is zero everywhere, i.e. $\omega(y,0)=0$. At $t=0^+$, a large velocity gradient is suddenly imposed at $y=0$. Since there is no change of velocity in any other direction, it follows that $\omega_z=\frac{\partial u}{\partial y}$. The sudden acceleration of the plate to a constant velocity, U, also suggests that the vorticity imposed at the boundary, i.e. at $y=0$, has the form of an *impulse load*.

Physically, a fixed amount of vorticity is introduced to the fluid in the form of a vortex sheet along the infinitely long plate. This amount is then diffused into the positive y direction while the total amount of vorticity remains constant. It was shown in section 3.6 that the solution to this problem is given by

$$\omega_z(y,t)=-\frac{U}{\sqrt{\pi\nu t}}e^{-\frac{y^2}{4\nu t}} \tag{7.54}$$

The solution is plotted in Fig. 7.19. At $t=0^+$, the vorticity is infinitely negative at the plate. At larger times, however, the vorticity diffuses gradually away from the plate while the area under each curve remains constant. This leads to a lower negative peak of vorticity at the plate that eventually approaches zero at very large times. Notice that in the figure the vorticity is converted to a dimensionless variable ω_* by dividing the local vorticity by $U/\sqrt{\pi\nu t_0}$, i.e. the maximum vorticity value, which is achieved at $y=0$ and $t=t_0$. The dimensionless distance is simply given by $\eta=y/\sqrt{4\nu t}$.

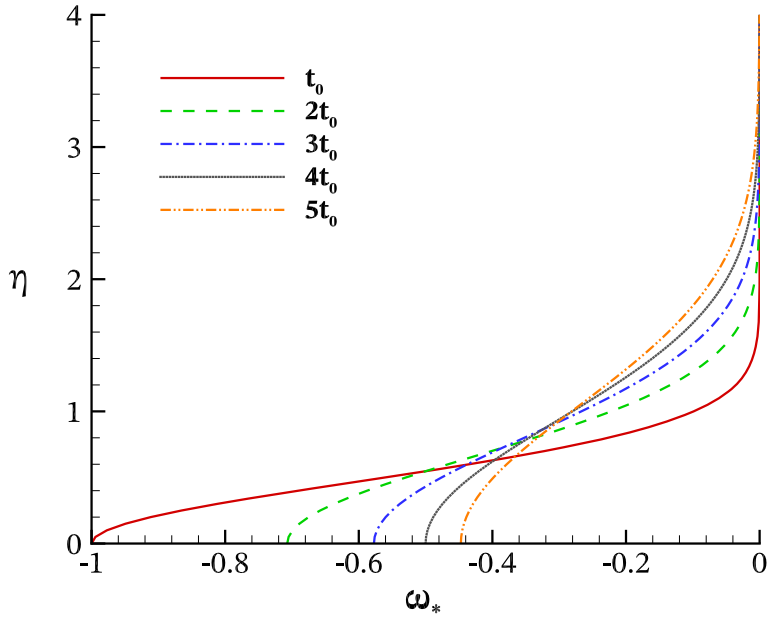

FIGURE 7.19 Vorticity profiles for accelerated plate

7.6.2 Vortex Shedding

The phenomenon of vortex shedding, of which a laboratory photograph is shown in Fig. 9.18, can be partially explained using the concepts of vortex stretching and diffusion, and a simplified analysis of the vorticity equation, i.e. Eq. (7.49), written as follows

$$\frac{\partial \boldsymbol{\omega}}{\partial t} + (\mathbf{V} \cdot \boldsymbol{\nabla})\, \boldsymbol{\omega} = \nu \boldsymbol{\nabla}^2 \boldsymbol{\omega} \tag{7.55}$$

This gives a relationship between the frequency of vortex fluctuation or shedding, f, and the assembly, advection and dissipation of vortices. If $\Delta\boldsymbol{\omega}$ is the scale of the vorticity fluctuations, then an order of magnitude statement based on Eq. (7.55) can be written as follows

$$f\,\Delta\boldsymbol{\omega} = c_1 U \frac{\Delta\boldsymbol{\omega}}{L} - c_2 \nu \frac{\Delta\boldsymbol{\omega}}{L^2} \tag{7.56}$$

where L is the length scale of the problem, e.g. the diameter of the blunt body responsible for the vortex shedding, and c_1 and c_2 are dimensionless constants. The signs of these constants are chosen by physical reasoning in order to make the expression compatible with the empirical Strouhal-Reynolds relation shown in Fig. 5.23. Notice that the fluctuations in vorticity increase due to the assembly part of the advective term, and decrease due to viscous dissipation. Therefore, division of Eq. (7.56) by $\Delta\boldsymbol{\omega} U/L$ leads to the following relation

$$\frac{fL}{U} = c_1 - c_2 \frac{\nu}{UL} \tag{7.57}$$

For intermediate values of the Reynolds number, the empirical constants are typically estimated as $c_1 = 0.212$ and $c_2 = 2.7$ (Ponta and Aref, 2004). This estimate is in good agreement with the measured data for the relationship between the Strouhal number, which is the dimensionless shedding frequency, and the Reynolds number, as was shown in Fig. 5.23 for flow past a circular cylinder. Further details on the frequency of vortex shedding can be found in texts on vortex dynamics (Wu et al., 2005).

7.6.3 Vortex Lines "Frozen in the Fluid"

The concepts of vorticity and circulation, already introduced in sections 7.1.1 and 7.2.3 play an important role in understanding how ideal fluid flow is related to viscous, rotational flow. By isolating vortex lines and vortex tubes in an otherwise irrotational flow field, we are able to study the behavior of vortex structures without the complications of viscosity or density variations, except for those due to pressure. Thus, for an inviscid, incompressible and barotropic fluid flowing under the influence of gravity, the vorticity equation, i.e. Eq. (7.50)

can be further simplified as follows

$$\frac{D\boldsymbol{\omega}}{Dt} = (\boldsymbol{\omega} \cdot \nabla)\,\mathbf{V} \tag{7.58}$$

Therefore, even for an inviscid fluid, the vorticity of fluid particles is not conserved because of the tilting and stretching of vortex lines. To shed additional light on this behavior, we rewrite Eq. (7.58) in index notation, as follows

$$\frac{D\omega_i}{Dt} = \omega_j \frac{\partial u_i}{\partial x_j} \tag{7.59}$$

The index form helps visualize what happens to a vortex tube, as it moves with the fluid. If for simplicity we focus on a single Cartesian component of Eq. (7.59), we can write

$$\frac{D\omega_x}{Dt} = \omega_x \frac{\partial u}{\partial x} + \omega_y \frac{\partial u}{\partial y} + \omega_z \frac{\partial u}{\partial z} \tag{7.60}$$

Thus, the partial derivatives of u act as coefficients of the corresponding components of vorticity. For example, if the fluid is accelerating in the x direction, the corresponding component of vorticity is strengthened, and the vortex tube is stretched in the x direction. Similarly, acceleration in the y or z directions intensifies those components of vorticity that tend to twist the vortex tube. To understand how a vortex line moves in a flow field, it is useful to compare it to a material line, i.e. a line that connects material particles in the fluid.

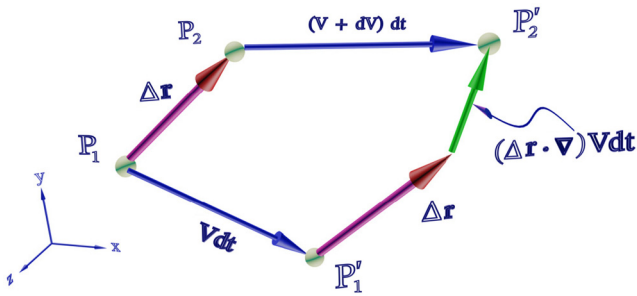

FIGURE 7.20 Evolution of a vector connecting two fluid particles

Consider, for example, two fluid particles P_1 and P_2 with position vectors $\mathbf{r}_1$ and $\mathbf{r}_2$, respectively. Let the particles be separated by a small distance $\Delta\mathbf{r}$, and then allow them to flow freely with the fluid. After an infinitesimally small time increment Δt, the particles find themselves at positions P'_1 and P'_2, as shown in Fig. 7.20. To track the evolution of $\Delta\mathbf{r}$ with time, we need to compute its

material derivative, i.e.

$$\begin{aligned}\frac{D}{Dt}(\Delta\mathbf{r}) &= \frac{D\mathbf{r}_2}{Dt} - \frac{D\mathbf{r}_1}{Dt} \\ &= \mathbf{V}(\mathbf{r}_2) - \mathbf{V}(\mathbf{r}_1)\end{aligned} \tag{7.61}$$

where $\mathbf{V}(\mathbf{r}_1)$ and $\mathbf{V}(\mathbf{r}_2)$ are the velocities of the two particles. Since the distance $\Delta\mathbf{r}$ is small, we can expand $\mathbf{V}(\mathbf{r}_2)$ about $\mathbf{V}(\mathbf{r}_1)$ in a Taylor series, and retain only the first order term, as follows

$$\begin{aligned}\frac{D}{Dt}(\Delta\mathbf{r}) &\simeq [\mathbf{V}(\mathbf{r}_1) + (\Delta\mathbf{r}\cdot\nabla)\,\mathbf{V}] - \mathbf{V}(\mathbf{r}_1) \\ &= (\Delta\mathbf{r}\cdot\nabla)\,\mathbf{V}\end{aligned} \tag{7.62}$$

where the gradient of $\mathbf{V}$ is computed according to Eq. (2.13). Therefore, Eq. (7.62) can also be written in index notation, as follows

$$\frac{D}{Dt}(\Delta r_i) = \Delta r_j \frac{\partial u_i}{\partial x_j} \tag{7.63}$$

Comparison of Eq. (7.58) with Eq. (7.62) or Eqs. (7.59) with (7.63) shows that the evolution of a vortex line follows the same rule as the evolution of the displacement vector between two fluid particles, which is a differential element of a material line. This implies that in a continuous velocity field, vortex lines remain continuous, i.e. they may twist and stretch, but they cannot be torn apart.

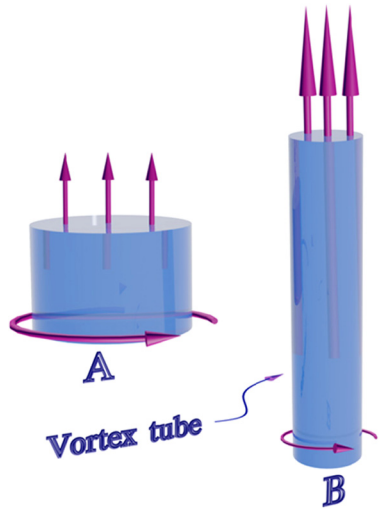

FIGURE 7.21 Stretching of vortex tube

Furthermore, if a vortex line coincides with a material line at one time, the two lines remain frozen together at later times as well. Since material lines move

with the fluid, we say that vortex lines are *frozen in the fluid*. The physical implications of this are significant for the evolution of vorticity. As shown in Fig. 7.21, stretching of material lines results in intensification of vorticity. However, mass conservation requires that the material lines become more squeezed together, and the surface of the associated stream tube shrinks. This allows the circulation to remain constant, as the vorticity is now integrated over a smaller material surface.

The preceding discussion leads to the conclusion that, in the limit, vortex stretching and vorticity intensification may tend to infinity. In most natural vortices occurring in the environment, however, vortex stretching is balanced by the viscous term in the vorticity transport equation, which we neglected in the present analysis. As the swirling of the flow increases, the velocity increases as well, and the same is true for viscous dissipation. Thus, a balance between vortex stretching and dissipation is finally achieved, and the vortex maintains a finite diameter, as it is common for tornadoes, water spouts, and similar naturally occurring vortices.

7.7 VORTICITY THEOREMS

The intricate relation between vorticity and circulation is captured by a series of important theorems of classical hydrodynamics that historically preceded the formulation of viscous flow. These theorems outline the limits of applicability of ideal fluid flow, and highlight the significance of the underlying assumptions.

7.7.1 Stokes' Theorem

Vorticity and circulation are related by a major kinematical concept known as Stokes' theorem. It states that the line integral of the tangential component of a vector field around a piece-wise smooth, closed curve, L, is equal to the surface integral of the normal component of the curl of the vector field over the surface bounded by L. Therefore

$$\Gamma = \oint_L \mathbf{V} \cdot \mathbf{t}\, dL = \int_S \nabla \times \mathbf{V} \cdot \mathbf{n}\, dS \tag{7.64}$$

Specifically, the circulation, defined by Eq. (7.8), is equal to the integral of the normal component of the vorticity over the surface bounded by the curve along which the circulation is computed. A formal proof of Stokes' theorem is beyond the scope of this book, but some intuitive arguments can provide a good grasp of the theorem's argument. Referring to Fig. 7.22, let us subdivide the surface S into small elements, which are approximately rectangular, and have their sides oriented along the coordinate axes x and y. Then, the normal to the surface, $\mathbf{n}$, is identical to the unit vector $\mathbf{k}$ in the z direction and

$$\nabla \times \mathbf{V} \cdot \mathbf{n} = \frac{\partial v}{\partial x} - \frac{\partial u}{\partial y} \tag{7.65}$$

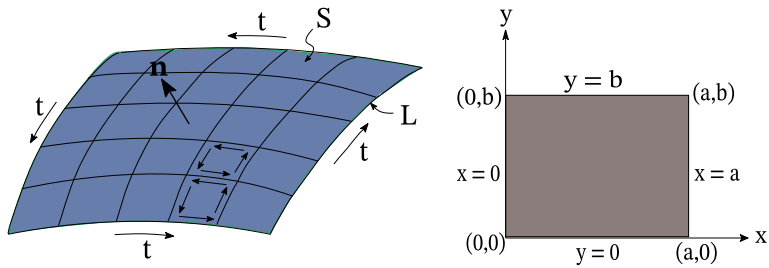

FIGURE 7.22 Definition sketch for Stokes' theorem

Therefore, the surface integral in Eq. (7.64) can be written as follows

$$\int_S \left(\frac{\partial v}{\partial x} - \frac{\partial u}{\partial y} \right) dx\, dy = \int_0^b \int_0^a \frac{\partial v}{\partial x}\, dx\, dy - \int_0^a \int_0^b \frac{\partial u}{\partial y}\, dy\, dx$$
$$= \int_0^a u(x, 0)\, dx + \int_0^b v(a, y)\, dy + \int_a^0 u(x, b)\, dx + \int_b^0 v(0, y)\, dy \tag{7.66}$$

This is identical to the line integral of **V** around the rectangle. If we sum all the surface integrals corresponding to the elementary rectangles in Fig. 7.22, the result is identical to the right hand side of Eq. (7.64). If we sum all of the line integrals, all internal circulations cancel out, and the left hand side of Eq. (7.64) follows. Therefore, assuming that the foregoing decomposition is possible, Stokes' theorem can be given a simple physical meaning.

7.7.2 Vortex Strength Theorem

As described in section 7.2.3, the strength of a vortex is determined by the circulation in a closed loop around the curvilinear surface of the associated vortex tube. It is therefore important to determine how the strength of a vortex varies along its axis, as the vortex is carried through the fluid while being stretched and twisted. To this purpose, let us consider the curvilinear side surface of a vortex tube with an infinitesimally narrow strip removed, as shown in Fig. 7.23. The gap between points A and D is negligible, but still the line integral cannot be carried out in that direction. The same is true for points B and C. Therefore, we need to compute the circulation around the perimeter of this surface by integrating the tangential component of the velocity along the path $ABCDA$, as shown by the arrows in Fig. 7.23. Then, the circulation can be computed as follows

$$\begin{aligned}\Gamma &= \oint_{ABCDA} \mathbf{V}\cdot\mathbf{t}\,dL \\ &= \int_{AB} \mathbf{V}\cdot\mathbf{t}\,dL + \int_{BC} \mathbf{V}\cdot\mathbf{t}\,dL + \int_{CD} \mathbf{V}\cdot\mathbf{t}\,dL + \int_{DA} \mathbf{V}\cdot\mathbf{t}\,dL\end{aligned} \tag{7.67}$$

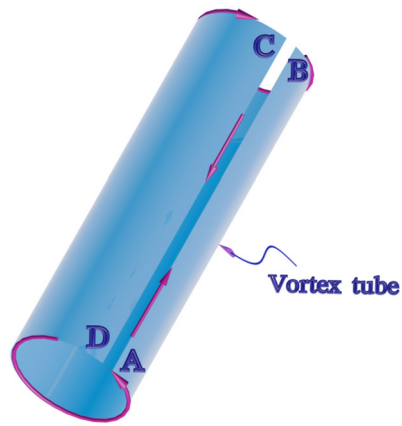

FIGURE 7.23 Vortex side surface

Notice, however, that the line integrals along AB and CD are exactly equal in magnitude but of opposite sign, thus they cancel out. Therefore, the circulation

is given by

$$\Gamma = \oint_{BC} \mathbf{V} \cdot \mathbf{t} dL + \oint_{DA} \mathbf{V} \cdot \mathbf{t} dL \tag{7.68}$$

According to Stokes' theorem, the circulation around the surface $ABCDA$ is equal to the normal flux of vorticity through this surface. However, the surface is made of vortex lines, thus by definition, the vorticity flux is zero. Therefore, the circulation around $ABCDA$ is also zero, i.e.

$$\oint_{BC} \mathbf{V} \cdot \mathbf{t} dL = \oint_{AD} \mathbf{V} \cdot \mathbf{t} dL \tag{7.69}$$

since the integration along AD and BC was carried out in the reverse direction. We conclude that the circulation is the same in all circuits embracing any vortex tube, i.e. the strength of a vortex is constant. This is known as the *vortex strength theorem* or *Helmholtz's first theorem*, named after Hermann von Helmholtz (1821–1894), a German physicist who made significant contributions to modern science and engineering.

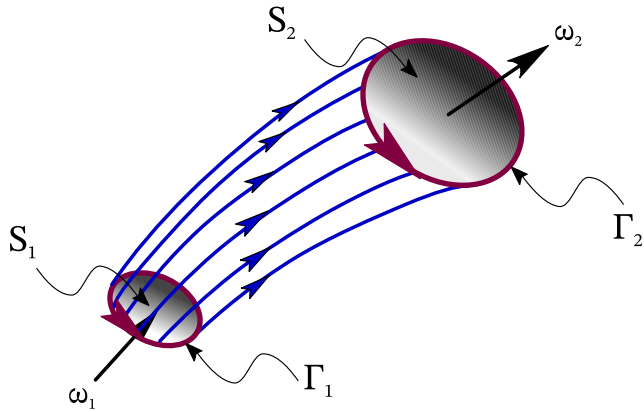

FIGURE 7.24 Vorticity fluxes

7.7.3 Vortex End Theorem

There are some physical implications regarding vortices in steady flow that follow immediately from the vortex strength theorem. Referring to Fig. 7.24, the circulation around the two circuits shown is the same, i.e. $\Gamma_1 = \Gamma_2$. Now, let us invoke Stokes' theorem once again. It states that the vorticity flux normal to the cross-sectional areas S_1 and S_2 is equal to the corresponding circulation, thus the vorticity fluxes through these surfaces are equal, i.e.

$$\int_{S_1} \boldsymbol{\omega} \cdot \mathbf{n} dS = \int_{S_2} \boldsymbol{\omega} \cdot \mathbf{n} dS \tag{7.70}$$

Eq. (7.70) is a statement of conservation of vorticity through a vortex tube. For example, if ω_1 and ω_2 are the average values of vorticity through S_1 and S_2, respectively, then

$$\omega_1 S_1 = \omega_2 S_2 \tag{7.71}$$

Therefore, as the cross-sectional area of a vortex increases, the vorticity must decrease and vice versa. This has significant implications on vortex stretching, i.e. the self-induced elongation of vortices along their axis, which was predicted by Eq. (7.55).

Thus, when a vortex is stretched, its vorticity in the direction of stretching increases according to Eq. (7.70). Furthermore, $\Gamma = \omega S$ is constant, and since the vortex tube is a material volume, its volume $\mathcal{V}$ is also constant. Then the ratio of vortex tube circulation to its volume is also constant, i.e.

$$\frac{\Gamma}{\mathcal{V}} = \frac{\omega}{L} = \text{constant} \tag{7.72}$$

where L is the length of the vortex tube. As L increases, ω must increase as well while the radius of the vortex tube decreases.

Because of the conservation of vorticity along a vortex tube, a vortex cannot end inside the fluid domain. Instead, a vortex must either extend to infinity or end on a solid boundary or a free surface. This behavior is known as the *vortex end theorem* or Helmholtz's second theorem. There are some notable exceptions to the vortex end theorem when applied to real fluids. For example, a vortex tube cannot terminate on a solid surface on which the no-slip condition is enforced.

As the vortex tube approaches a stationary boundary, Eq. (7.70) requires that in theory the cross-sectional area of the vortex tube become infinitely large. However, resistance at the boundary prevents this from happening, and further expansion of the vortex tube is limited by viscous dissipation. This is approximately the case when a water spout makes contact with the water surface.

A vortex can also form a closed loop, known as a *vortex ring*. Several vortex rings are shown in Fig. 7.25 formed by a pulsating water jet. The pulses have 20 ms duration at 85 intervals. The orifice diameter is 0.0254 m and the discharge velocity is 0.8 m/s. Nine small orifices were fitted around the vortex generator for dye injection to help visualized the rings.

Results of similar experiments on thin core rings generated by a piston gun in water are shown in Fig. 7.26, which uses hydrogen bubbles to identify the core. The vortex rings in the photograph are seen looking directly into the mouth of the gun. Notice the thin core and large-amplitude bending waves.

7.7.4 Helicity

The creation of vortex rings complicates the topology of vortices significantly, as these rings can become knotted or tangled during fluid motion. To obtain a measure of these features, we need to perform a geometric decomposition of the

vorticity vector with respect to the velocity vector, and vice versa. The approach is known as the *Helmholtz decomposition*, and applies to any vector field, but in the following we will focus the discussion on the velocity and vorticity vector fields.

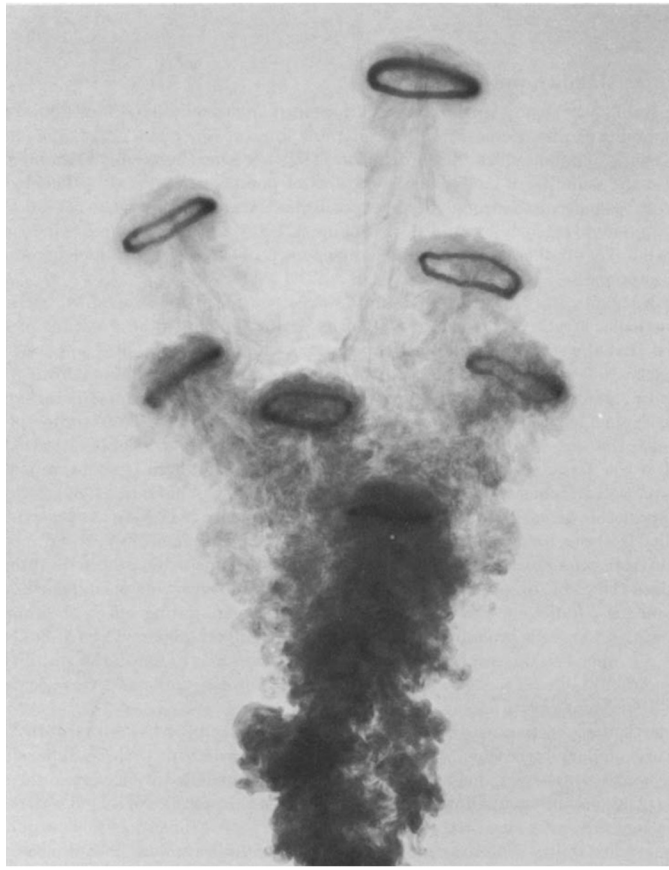

FIGURE 7.25 Vortex rings. Reproduced from Glezer (1981). Courtesy of Dr. Ari Glezer

To begin, let us recall the decomposition of an arbitrary vector in two components, one of which is parallel, and the other perpendicular to some unit vector, as described by Eq. (1.134). This operation can be repeated when the two vectors are $\mathbf{V}$ and $\boldsymbol{\omega}$, which leads to the following decompositions

$$\begin{aligned} |\mathbf{V}|^2 \boldsymbol{\omega} &= \mathbf{V}(\boldsymbol{\omega} \cdot \mathbf{V}) - \mathbf{V} \times (\mathbf{V} \times \boldsymbol{\omega}) \\ |\boldsymbol{\omega}|^2 \mathbf{V} &= \boldsymbol{\omega}(\boldsymbol{\omega} \cdot \mathbf{V}) - \boldsymbol{\omega} \times (\mathbf{V} \times \boldsymbol{\omega}) \end{aligned} \tag{7.73}$$

The two vector products that appear in Eq. (7.73) play a significant role in vorticity dynamics. The scalar product of velocity and vorticity, $h = \boldsymbol{\omega} \cdot \mathbf{V}$, is called

the *helicity density*. As its definition by means of the scalar product states, the helicity density is the stream-wise component of vorticity. The vector product of velocity and vorticity, $\boldsymbol{\omega} \times \mathbf{V}$, is called the *Lamb vector*. The latter can also be written as $2\boldsymbol{\Omega} \times \mathbf{V}$, and thus may be interpreted as the Coriolis acceleration of the velocity field under the effect of its own rotation. The Coriolis acceleration will be described in section 10.2.5 where the physical interpretation of the Lamb vector will become apparent. The integral of the helicity density over a flow domain $\mathcal{V}$ is called the *helicity*, and is defined as follows

$$\mathcal{H} = \int_{\mathcal{V}} \mathbf{V} \cdot \boldsymbol{\omega} d\mathcal{V} \tag{7.74}$$

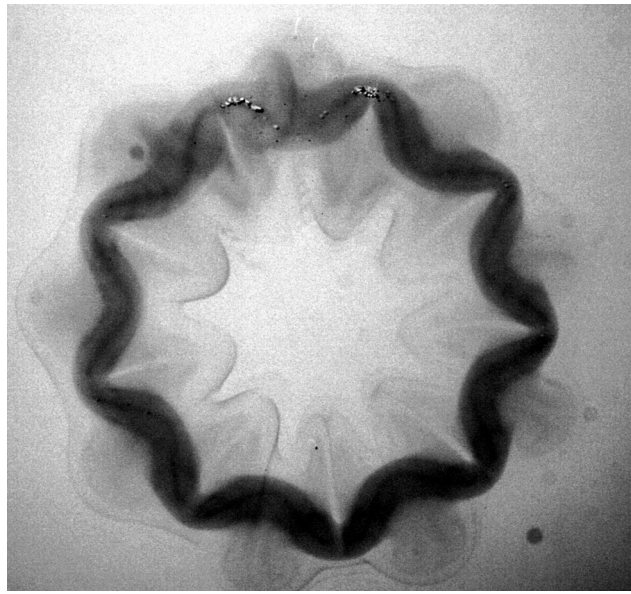

FIGURE 7.26 Vortex ring. Reproduced from Sullivan et al. (2008) with permission from Cambridge University Press

Helicity is a flow property which represents the potential for helical flow to develop. The term helicity was introduced by Moffatt to describe flows whose streamlines are helical in shape, and is a measure of the linked-ness and knotted-ness of the flow (Moffatt, 1969). In common flow problems, such as shear flow in a channel, it is difficult to imagine how the vorticity could attain a component in the stream-wise direction. However, there are numerous examples of non-zero helicity in environmental fluid mechanics. These include flow in a river bend, flow in braided channels, the updraft flow in a thunderstorm, and many others. The analysis of helical flows is beyond the scope of this book, thus the interested reader is referred to specialized texts on vorticity dynamics (Truesdell, 1954). In

the following, we present a simple example adopted from the article by Moffat and Tsinober (1992).

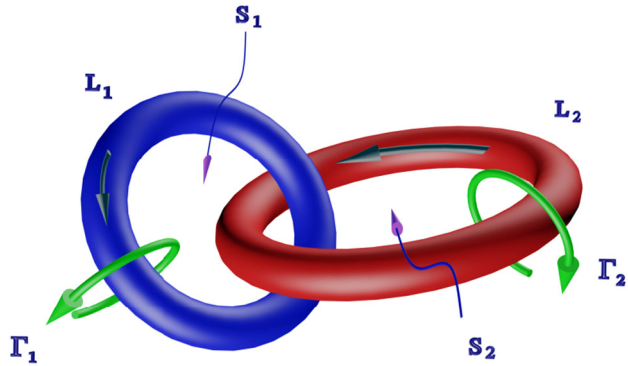

FIGURE 7.27 Linked vortex tubes

Consider two thin ring vortices with axes L_1 and L_2 in an otherwise irrotational flow domain, as shown in Fig. 7.27. The vortices are linked together and have volumes $\mathcal{V}_1$ and $\mathcal{V}_2$, and cross-sectional areas A_1 and A_2, respectively. The vortex lines within each vortex tube are un-knotted and un-twisted closed curves passing once around the tube. Furthermore, there is no linking among the vortex lines. The arrows drawn on the tubes show the direction of the vorticity. If we assume now that the cross-sectional area of the two tubes is very small, the surfaces enclosed by the axes L_1 and L_2 have the shape of two disks with areas S_1 and S_2, respectively. Finally, the constant strength of the two vortices is represented by their circulations Γ_1 and Γ_2, respectively.

Since the rest of the domain is irrotational, the helicity in the flow domain only involves the volumes of the two vortex tubes. Then, the helicity can be computed from the sum of the volume integrals over each vortex tube, i.e.

$$\mathcal{H} = \int_{\mathcal{V}_1} \mathbf{V} \cdot \boldsymbol{\omega} d\mathcal{V}_1 + \int_{\mathcal{V}_2} \mathbf{V} \cdot \boldsymbol{\omega} d\mathcal{V}_2 \tag{7.75}$$

Since the vortices are uniform, we can re-write these integrals as follows

$$\mathcal{H} = \oint_{L_1} \mathbf{V} \cdot \left(\int_{A_1} \boldsymbol{\omega} dA_1 \right) \mathbf{t} dl_1 + \oint_{L_2} \mathbf{V} \cdot \left(\int_{A_2} \boldsymbol{\omega} dA_2 \right) \mathbf{t} dl_2 \tag{7.76}$$

where $\mathbf{t}$ is the vector tangent to the vortex axis. As a result of Stokes' theorem, the area integrals in parenthesis are equal to the corresponding circulation, thus we can further write

$$\mathcal{H} = \Gamma_1 \oint_{L_1} \mathbf{V} \cdot \mathbf{t} dl_1 + \Gamma_2 \oint_{L_2} \mathbf{V} \cdot \mathbf{t} dl_2 \tag{7.77}$$

Notice, however, that the line integrals around L_1 and L_2 are equal to the vorticity flux through the enclosed areas S_1 and S_2, respectively. Therefore, Eq. (7.77) can be written as follows

$$\mathcal{H} = \Gamma_1 \int_{S_1} \boldsymbol{\omega} \cdot \mathbf{n}_1 dS_1 + \Gamma_2 \int_{S_2} \boldsymbol{\omega} \cdot \mathbf{n}_2 dS_2 \tag{7.78}$$

where $\mathbf{n}_1$ and $\mathbf{n}_2$ are the unit normal vectors to the areas S_1 and S_2, respectively. However, S_1 has zero vorticity flux everywhere except where vortex tube $\mathcal{V}_2$ crosses it. Similarly, S_2 has zero vorticity flux everywhere except where vortex tube $\mathcal{V}_1$ crosses it. Those fluxes are of course equal to the circulation around these tubes, therefore Eq. (7.78) can be finally written as follows

$$\mathcal{H} = 2\Gamma_1\Gamma_2 \tag{7.79}$$

The sign of the helicity is determined by the direction of the vorticity vectors within the two tubes. If, for example, the direction of one vortex tube were reversed, the sign of Eq. (7.79) would become negative. If the direction in both vortex tubes is reversed, the sign will return to positive. Furthermore, if additional links were added or the links became knotted, the same basic principles would apply. The topology becomes complicated, however, and the analytical evaluation of helicity becomes complicated. Finally, if there are no links between the vortex rings, the helicity would vanish.

What causes vortex filaments to tilt and produce helical flow patterns is not immediately obvious. In the simplest possible explanation, either topography, external rotation, or a convective updraft due to uneven heating may cause a secondary current which rotates the fluid, so that the rotation vector points in the direction of mean flow. The most severe consequences of non-zero helicity in environmental flows are found when vortex lines are tilted in the direction of flow creating high levels of stream-wise vorticity in a thunderstorm. In such cases, helicity may be used as a measure of the intensity of rotation in a thunderstorm's updraft. High helicity values, typically more than 200 m^2/s^2, favor the development of mid-level rotation, which indicates that the storm may become a super-cell and produce a tornado (Lemon and Doswell, 1979, Davies-Jones, 1984).

7.7.5 Enstrophy

The kinetic energy is a well-accepted measure of the intensity of a velocity field, thus it is natural to seek a similar measure for the intensity of the vorticity field. We define the *enstrophy density* as half the squared magnitude of the vorticity vector, i.e.

$$Z = \frac{1}{2}(\boldsymbol{\omega} \cdot \boldsymbol{\omega}) = \frac{1}{2}\omega_i \omega_i \tag{7.80}$$

Enstrophy is a fundamental flow property that describes the fluid's ability to dissipate its kinetic energy. Enstrophy is particularly useful in the study of turbulent flows, and has some interesting properties in two-dimensional flow applications. To obtain an equation for the evolution of enstrophy density, we take the scalar product of the vorticity equation for incompressible flow, i.e. Eq. (7.51), with the vorticity vector, as follows

$$\frac{DZ}{Dt} = \omega_i \omega_j \frac{\partial u_i}{\partial x_j} + \frac{\omega_i}{\rho^2} \epsilon_{ijk} \frac{\partial \rho}{\partial x_j} \frac{\partial p}{\partial x_k} + \nu \omega_i \frac{\partial^2 \omega_i}{\partial x_j \partial x_j} \tag{7.81}$$

The first term on the right hand side contains the familiar velocity gradient tensor described by Eq. (5.69). Therefore, we can expand the term in question as follows

$$\begin{aligned} \omega_i \omega_j \left(S_{ij} + \Omega_{ij} \right) &= \omega_i \omega_j S_{ij} + \frac{1}{2} \omega_i \omega_j \left(\frac{\partial u_i}{\partial x_j} - \frac{\partial u_j}{\partial x_i} \right) \\ &= \omega_i \omega_j S_{ij} + \frac{1}{2} \left(\omega_i \omega_j \frac{\partial u_i}{\partial x_j} - \omega_i \omega_j \frac{\partial u_j}{\partial x_i} \right) \\ &= \omega_i \omega_j S_{ij} \end{aligned} \tag{7.82}$$

Thus, the first term on the right hand side of Eq. (7.81) can be written in terms of the strain rate tensor alone. If in addition we omit the baroclinic term for simplicity, Eq. (7.81) can be simplified as follows

$$\frac{DZ}{Dt} = \omega_i \omega_j S_{ij} + \nu \omega_i \frac{\partial^2 \omega_i}{\partial x_j \partial x_j} \tag{7.83}$$

The first term on the right hand side represents the production of enstrophy by the strain rate while the second stands for the viscous destruction of enstrophy. Notice that strictly speaking we cannot consider this term as a dissipation process because enstrophy is not invariant when the fluid is inviscid. In summary, when a fluid element is stretched, its enstrophy will increase. Thus, when the vorticity is subject to a strain rate tensor leading to elongation of fluid elements, the enstrophy may become very intense. In addition, the vortex tilting mechanism can make the field of enstrophy very complicated.

In two-dimensional flow applications, e.g. flow in a shallow channel where the flow is entirely on the $x-z$ plane, and is therefore independent of the vertical coordinate, y, the vorticity dynamics is drastically altered. The vorticity vector is purely vertical, i.e. $\boldsymbol{\omega} = \omega_y \mathbf{j}$. As a result, the enstrophy production term becomes

$$\omega_i \omega_j S_{ij} = \omega_y^2 S_{yy} = \omega_y^2 \frac{\partial v}{\partial y} \tag{7.84}$$

However, the continuity equation requires that

$$\frac{\partial u}{\partial x} + \frac{\partial w}{\partial z} = 0 \tag{7.85}$$

Therefore, we must also have $\frac{\partial v}{\partial y} = 0$, and the enstrophy production term vanishes. This means that in two-dimensional flow, the enstrophy will decay monotonically, i.e. the evolution of enstrophy obeys a simple diffusion process of the following form

$$\frac{DZ}{Dt} = \nu\omega_i \frac{\partial^2 \omega_i}{\partial x_j \partial x_j} \tag{7.86}$$

Finally, if viscous effects become negligible, $\frac{DZ}{Dt} = 0$, therefore the enstrophy of two-dimensional, inviscid flows is conserved.

7.7.6 Kelvin's Circulation Theorem

We are now in a position to study the temporal changes in circulation around a space curve moving with the fluid velocity. The curve is by definition a material curve, therefore it consists of the same fluid particles at all times.

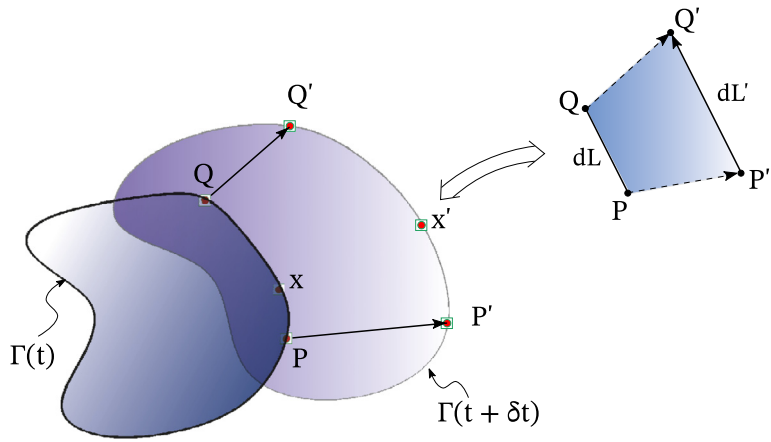

FIGURE 7.28 Time variation of a material curve

We first consider only a small segment of the closed curve, identified in Fig. 7.28 by PQ. An increment of time later, the segment is represented by $P'Q'$. Thus, differentiation of Eq. (7.8) with respect to time leads to

$$\frac{d}{dt}\int_P^Q V_t(x_i, t)\, dL = \lim_{\delta t \to 0} \frac{1}{\delta t}\left\{\int_{P'}^{Q'} V_t(x_i', t + \delta t)\, dL' - \int_P^Q V_t(x_i, t)\, dL\right\} \tag{7.87}$$

in which V_t is the tangential component of velocity, and x_i' is the new location of an arbitrary point x_i, after a time increment δt has elapsed. If the distance

PQ is infinitesimal, this can be simplified as follows

$$\frac{d}{dt}\int_P^Q V_t(x_i,t)\,dL = \lim_{\delta t\to 0}\frac{1}{\delta t}\left\{V_t(x_i',t+\delta t)\overrightarrow{P'Q'} - V_t(x_i,t)\overrightarrow{PQ}\right\} \tag{7.88}$$

At the end of the time increment δt, the new value of velocity has been affected by two different processes which can be quantified by a Taylor series expansion. First, temporal acceleration results in

$$V_t(x_i,t+\delta t) = V_t(x_i,t) + \frac{\partial V_t}{\partial t}(x_i,t)\delta t + \cdots \tag{7.89}$$

Next, convective acceleration along the travel path leads to

$$V_t(x_i',t+\delta t) = V_t(x_i,t+\delta t) + (\overrightarrow{PP'}\cdot\nabla)V_t(x_i,t+\delta t) + \cdots \tag{7.90}$$

Since the curve moves with the fluid velocity, the vector $\overrightarrow{PP'}$ is simply the distance traveled by fluid particles, i.e.

$$\overrightarrow{PP'} = \mathbf{V}(x_i,t)\delta t + \cdots \tag{7.91}$$

Now, both the velocity $\mathbf{V}$ and the boundary curve segment $\overrightarrow{P'Q'}$ change with time. The new length of the segment is given by the stretching due to the velocity variation along the segment

$$\overrightarrow{P'Q'} = \overrightarrow{PQ} + \left(\overrightarrow{PQ}\cdot\nabla\right)\mathbf{V}(x_i,t)\delta t + \cdots \tag{7.92}$$

Substitution of Eqs. (7.89) through (7.91) in Eq. (7.87) and truncation of terms higher than first order in δt yields

$$\lim_{\delta t\to 0}\frac{1}{\delta t}\left[V_t(x_i',t+\delta t)\overrightarrow{P'Q'} - V_t(x_i,t)\overrightarrow{PQ}\right] = \frac{\partial V_t}{\partial t} + (\mathbf{V}\cdot\nabla)V_t\overrightarrow{PQ} + V_t(\overrightarrow{PQ}\cdot\nabla)\mathbf{V} \tag{7.93}$$

Now, as the segment PQ and the time increment δt shrink to dL and dt, respectively, the integral in Eq. (7.87) becomes

$$\frac{d\Gamma}{dt} = \oint\frac{D\mathbf{V}}{Dt}\cdot\mathbf{t}\,dL + \oint\mathbf{V}\cdot(\mathbf{t}\cdot\nabla)\mathbf{V}\,dL \tag{7.94}$$

Eq. (7.94) shows that once the material curve is specified, the circulation is only a function of time. Its time derivative, on the other hand, depends both on the variation of $\mathbf{V}$, and on the changes in shape and orientation of the material curve.

The material derivative of velocity appearing in Eq. (7.94) can be replaced by means of the forces on the right hand side of Eq. (5.48). Then, if the second integral on the right is grouped together with the pressure and gravitational forces, Eq. (7.94) can be written as follows

$$\frac{d\Gamma}{dt} = -\frac{1}{\rho}\oint \frac{\partial}{\partial x_i}\left(p + \gamma\zeta + \rho\frac{V^2}{2}\right) t_i\, dL + \frac{1}{\rho}\oint \frac{\partial \tau_{ji}}{\partial x_j} t_i\, dL \tag{7.95}$$

in which t_i are the components of the unit vector tangent to the closed curve L. It can be seen that for single-valued gravitational, velocity and pressure fields, the first closed integral on the right vanishes. A rare exception can occur if a non-conservative body force is present, like the Coriolis force, or pressure-density forces, as in baroclinic flows, but we need not worry about such problems in the present context. If in addition, we have reasons to believe that shear stresses can be neglected, the circulation around a material curve remains constant with time. In turn, by virtue of Stokes' theorem, the vorticity of any fluid element cannot change with time if the deformation stresses are negligible. This very important statement, known as *Helmholtz's circulation theorem* (Helmholtz, 1858), allows significant simplification of a great number of problems in which the initial vorticity is nearly zero. Then, if the viscous stresses are neglected, an assumption which is justified in many problems, the flow can be considered as irrotational throughout the solution. Since a great deal of problems begin from initial conditions involving a fluid at rest, and therefore having zero vorticity, negligible viscous stresses will allow the condition of irrotationality to remain true during the entire course of the solution.

It should be mentioned that the circulation theorem of Helmholtz is often derived as an extension of *Kelvin's circulation theorem*. William Thomson, also known as Lord Kelvin (1824–1907) was an Irish physicist and engineer who made major contributions to thermodynamics and mechanics. His theorem states that for an ideal fluid, i.e. inviscid and irrotational, under the action of conservative forces, e.g. gravity, the circulation around any closed material curve is constant. There is evidence of correspondence between the two scientists, and although Helmholtz published his results in 1858, well in advance of the publication of Kelvin's theorem in 1867, it is believed that Kelvin's suggestion was the basis of Helmholtz's theorem.

The influence of viscous stresses begins to diminish at high Reynolds numbers, thus a class of problems exists that are both irrotational and inviscid. It should be mentioned, however, that the requirement of an inviscid fluid is too strong to assure the condition of irrotationality. In fact many interesting cases of irrotational flow of a viscous fluid exist, and the interested reader is directed to some excellent treatises on the subject (Joseph et al., 2008).

7.7.7 Conservation of Helicity

A vortex tube is a material volume that moves with the fluid in such a manner that the vorticity vector remains tangent to the surface of the tube. According to Stokes' theorem, this implies that the circulation, and thus the strength of the vortex tube remain uniform along the tube. Helmholtz's circulation theorem further clarifies the evolution of a vortex tube by stating that its strength remains constant in time, if the fluid is inviscid, and all the body forces acting on it are conservative, as is the case for gravity. Therefore, vortex lines behave like material lines and, as it was shown earlier, they are frozen in the fluid. Furthermore, if the vortex line is closed as to form a vortex ring, then the vorticity is conserved.

Consider now a material volume, $\forall$, enclosed by a surface, S, which is also moving with the fluid. Let the vorticity vector be everywhere tangent to the surface S, so that $\boldsymbol{\omega} \cdot \mathbf{n} = 0$, where $\mathbf{n}$ is the unit normal vector to the surface S. We are interested in investigating the evolution of the helicity contained in the volume $\forall$. This can be accomplished by evaluating the material derivative of the helicity, which can be written as follows

$$\frac{D\mathcal{H}}{Dt} = \int_{\forall} \frac{Dh}{Dt} d\forall \tag{7.96}$$

Next, the helicity density, h, can be written in terms of the vorticity and the velocity, i.e.

$$\begin{aligned} \frac{D\mathcal{H}}{Dt} &= \int_{\forall} \frac{D}{Dt} (\mathbf{V} \cdot \boldsymbol{\omega}) \ \rho d\forall \\ &= \int_{\forall} \left(\frac{D\mathbf{V}}{Dt} \cdot \boldsymbol{\omega} + \mathbf{V} \cdot \frac{D\boldsymbol{\omega}}{Dt} \right) \rho d\forall \end{aligned} \tag{7.97}$$

The material derivative in first term on the right hand side can be eliminated using Eq. (5.113), after neglecting the viscous term. Similarly, the material derivative in the second term on the right hand side can be eliminated by means of the vorticity evolution equation for a barotropic, inviscid fluid, i.e. Eq. (7.58). Therefore

$$\frac{D\mathcal{H}}{Dt} = \int_{\forall} \left[\left(\mathbf{g} - \frac{1}{\rho} \nabla p \right) \cdot \boldsymbol{\omega} + \mathbf{V} \cdot [(\boldsymbol{\omega} \cdot \nabla) \mathbf{V}] \right] d\forall \tag{7.98}$$

The gravitational force may be expressed as the gradient of the gravitational potential. This is given for any vector by Eq. (2.27), and is described for the gravitational potential in section 10.3. Thus, we can express the evolution of helicity as follows

$$\frac{D\mathcal{H}}{Dt} = \int_{\forall} \left\{ -\nabla \cdot \left[\left(\Phi + \frac{p}{\rho} \right) \boldsymbol{\omega} \right] + \nabla \cdot \left(\frac{V^2}{2} \boldsymbol{\omega} \right) \right\} d\forall \tag{7.99}$$

where $V = (\mathbf{V} \cdot \mathbf{V})^{1/2}$ is the magnitude of the velocity vector. Then, after collecting terms, we can write

$$\begin{aligned} \frac{D\mathcal{H}}{Dt} &= \int_{\mathcal{V}} \nabla \cdot \left[\left(\frac{V^2}{2} - \frac{p}{\rho} - \Phi \right) \boldsymbol{\omega} \right] d\mathcal{V} \\ &= \int_S \left(\frac{V^2}{2} - \frac{p}{\rho} - \Phi \right) (\boldsymbol{\omega} \cdot \mathbf{n})\, dS \\ &= 0 \end{aligned} \tag{7.100}$$

The conversion of the volume integral to a surface integral was made possible by the divergence theorem, as expressed by Eq. (2.103). Then, because by definition the normal derivative of the vorticity vanishes on the bounding surface S, the material derivative of the helicity is equal to zero. Thus, for an inviscid fluid, besides energy, helicity is conserved as well.

The conservation of helicity in inviscid flow is a remarkable discovery. It states that regardless of the complexity of the vorticity field, i.e. tilting, stretching, or any other distortion, the strength and topology of the vortex tubes are invariant. Conservation of helicity implies that as the flow evolves, these vortex tubes will preserve their identity, and the will not break or decay.

PROBLEMS

7-1. Consider the steady flow of a viscous fluid confined between two flat plates at a distance B apart. The upper plate is moving parallel to itself at speed U, and the lower plate is held stationary. Calculate the vorticity in the flow.

7-2. What is the difference between rigid body rotation and an irrotational vortex? Hint: Use a two-dimensional element to examine the differences and similarities of the two flow patterns.

7-3. In a major hurricane the maximum observed winds had a magnitude of 250 km/hr. The winds had diminished further out from the center, and at distance of 300 km an independent measurement found wind speeds of approximately 80 km/hr. Assuming that a Rankine vortex is a reasonable model of the wind field, describe the wind speed as a function of radial distance from the hurricane center.

7-4. In a variety of environmental problems, it is common to find fluid motions that have a cellular character; i.e. the fluid streamlines form closed loops in the form of a cell. An example of a 2D cellular flow is

$$\mathbf{u} = (u_x, u_y, 0) = (\sin \pi x \cos \pi y, -\cos \pi x \sin \pi y, 0)$$

- **a.** Calculate the vorticity.
- **b.** Indicate where the vorticity is highest, and where it vanishes.

7-5. For a barotropic fluid in a non-rotating reference frame, analyze the following flow conditions:

- **a.** If it is possible to develop vorticity in an inviscid flow for which the vorticity is initially zero everywhere.
- **b.** If it is possible to change the vorticity of an inviscid flow which does have vorticity initially.
- **c.** If it is possible for the fluid viscosity to cause diffusion of vorticity through the fluid from a region of high vorticity to regions where the flow was initially irrotational.

7-6. Analyze the flow, analogous to that in the soda-straw problem, for a column of fluid falling through a tube that has 90° bend.

7-7. Consider a fluid parcel undergoing a pure rigid-body rotation. Write the corresponding momentum equation, and show that the viscous term vanishes.

7-8. Consider a flow field described by a velocity $\mathbf{V}$ and a vorticity $\boldsymbol{\omega}$. Show that if ϕ is a material property, i.e. ϕ is conserved when moving with the fluid, then $\boldsymbol{\omega} \cdot \nabla\phi$ is also a material invariant property.

7-9. Explain the difference in the production of vorticity in an incompressible flow field and the flow of an incompressible fluid.

REFERENCES

Bénard, H., 1900. Les Tourbillons Cellulaires dans une Nappe Liquide. Revue Générale Des Sciences Pures Et Appliquées 11, 1261–1271.

Davies-Jones, R.P., 1984. Streamwise vorticity: the origin of updraft rotation. Journal of the Atmospheric Sciences 41, 2991–3006.

Falkovich, G., Sreenivasan, K.R., 2006. Lessons from hydrodynamic turbulence. Physics Today 59 (4), 43–49.

Fannjiang, A., Kiselevy, A., Ryzhik, L., 2006. Quenching of reaction by cellular flows. Geometric and Functional Analysis 16, 1261–1271.

Glezer, Ari, 1981. An Experimental Study of a Turbulent Vortex Ring. PhD thesis. California Institute of Technology.

Helmholtz, H., 1858. Über Integrale der Hydrodynamischen Gleichungen, welcher der Wirbelbewegungen Entsprechen (On integrals of the hydrodynamic equations which correspond to vortex motions). Journal für die Reine und Angewandte Mathematik 55, 25–55.

Joseph, D., Funada, T., Wang, J., 2008. Potential Flows of Viscous and Viscoelastic Fluids. Cambridge University Press.

Joukovsky, N.E., 1914. On the motion of water at a turn of a river. Matematicheskii Sbornik 28, 193–216. Reprinted in Collected Works 4. Moscow.

Lemon, L.R., Doswell, C.A., 1979. Severe thunderstorm evolution and mesocyclone structure as related to tornadogenesis. Monthly Weather Review 107, 1184–1197.

Moffat, H.K., Tsinober, A., 1992. Helicity in laminar and turbulent flow. Annual Review of Fluid Mechanics 24, 281–312.

Moffatt, H.K., 1969. The degree of knotted-ness of tangled vortex lines. Journal of Fluid Mechanics 36, 17–29.

Ponta, F.L., Aref, H., 2004. The Strouhal-Reynolds number relationship for vortex streets. Physical Review Letters 93, 084501.

Rayleigh, Lord, 1916. On convection currents in a horizontal layer of fluid, when the higher temperature is on the under side. Philosophical Magazine Series 6 32, 529–546.

Shapiro, A.H., 1969. Film Notes for Vorticity. National Committee on Fluid Mechanics Films.

Sullivan, I.S., Niemela, J.J., Hershberger, R.E., Bolster, D., Donnelly, R.J., 2008. Dynamics of thin vortex rings. Journal of Fluid Mechanics 609, 319–347.

Truesdell, C., 1954. The Kinematics of Vorticity. Indiana University Press, Bloomington, IN.

Wu, J.-Z., Ma, H.-Y., Zhou, M.-D., 2005. Vorticity and Vortex Dynamics. Springer, Berlin.